Available online at www.sciencedirect.com
ScienceDirect
Journal of Computational Physics 227 (2008) 2941–2969
JOURNAL OF COMPUTATIONAL PHYSICS
www.elsevier.com/locate/jcp

Modelling wave dynamics of compressible elastic materials

S.L. Gavrilyuk *, N. Favrie, R. Saurel

University Aix-Marseille, Polytech Marseille, UMR CNRS 6595 IUSTI, SMASH Project, INRIA, Institut Universitaire de France, 5 Rue E. Fermi, 13453 Marseille Cedex 13, France

Received 30 May 2007; received in revised form 19 November 2007; accepted 20 November 2007
Available online 4 December 2007

Abstract

An Eulerian conservative hyperbolic model of isotropic elastic materials subjected to finite deformation is addressed. It was developed by Godunov [S.K. Godunov, Elements of continuum mechanics, Nauka, Moscow, 1978 (in Russian) and G.H. Miller, P. Colella, A high-order Eulerian Godunov method for elastic–plastic flow in solids, J. Comput. Phys. 167 (2001) 131–176]. Some modifications are made concerning a more suitable form of governing equations. They form a set of evolution equations for a local cobasis which is naturally related to the Almansi deformation tensor. Another novelty is that the equation of state is given in terms of invariants of the Almansi tensor in a form which separates hydrodynamic and shear effects. This model is compared with another hyperbolic non-conservative model which is widely used in engineering sciences. For this model we develop a Riemann solver and determine some reference solutions which are compared with the conservative model. The numerical results for different tests show good agreement of both models for waves of very small and very large amplitude. However, for waves of intermediate amplitude important discrepancies between results are clearly visible.

Keywords: Conservative formulation; Riemann problem; Godunov method

1. Introduction

At least two types of hyperbolic models of elastic materials subjected to finite deformation can be found in the literature. The first one uses an evolution equation for the stress tensor (more exactly, for its traceless part). Such an approach is largely used in engineering science because it permits us to easily incorporate plasticity effects through Maxwell type relaxation models [19] mentioned that "their proponents suggest that these models are accurate even though they are thermodynamically inconsistent". Another drawback of such models is that they are not in conservative form. Hence, the definition of weak solution is questionable and, as a consequence, rigorous numerical resolution is problematic. Finally, the formulation of governing equations is somewhat phenomenological. Indeed, to satisfy the objectivity prin-

* Corresponding author.
E-mail addresses: sergey.gavrilyuk@polytech.univ-mrs.fr (S.L. Gavrilyuk), nicolas.favrie@polytech.univ-mrs.fr (N. Favrie), richard.saurel@polytech.univ-mrs.fr (R. Saurel).

0021-9991/$ - see front matter © 2007 Elsevier Inc. All rights reserved.
doi:10.1016/j.jcp.2007.11.030

ciple, Jaumann type derivatives should be used in the equation formulation, and this is not the only possible choice.

Another class of models deals with conservative hyperbolic thermodynamically consistent systems of equations formulated in terms of displacements [5,6,10,13,19]. The equations are supplemented by stationary conservation laws (differential constraints) compatible with the governing equations. The symmetrization of such mathematical models appearing in different areas of physics is discussed in [6]. The model we study here follows the lines of [5,10]. A modification is made concerning a more suitable form of governing equations. They are presented as a set of evolution equations for a local cobasis naturally related to the Almansi deformation tensor. This tensor is suitable for the Eulerian description of elastic isotropic materials. Another novelty is that the equation of state is given in terms of the invariants of the Almansi tensor in a form which separates hydrodynamic and shear effects under shock loading.

We compare the conservative model with a non-conservative hyperbolic model formulated in terms of the evolution equation for the deviator of the stress tensor [9,21].

The paper is organized as follows. In Section 2, we formulate a thermodynamically compatible non-conservative hyperbolic model. The structure of this model is such that it allows us to split governing equations into two subsystems. We develop an "exact" Riemann solver for such a system and obtain several reference solutions that will be used for comparison of the two models (conservative and non-conservative). In Section 3 we formulate an Eulerian conservative model in terms of a natural curvilinear basis associated with the Lagrangian coordinates. The hyperbolicity of this model is established. The equation of state is proposed in a form allowing separation of the energy into "hydrodynamic" and "elastic" parts compatible with the non-conservative model of Section 2. In Sections 4 and 5 we compare both models in a large domain of physical parameters. For the first non-conservative model we use an "exact" solution of the Riemann problem. For the second one we use a numerical solution by a second order Godunov method. An approximate HLLC type solver [17] was used. The numerical results for different tests show good agreement of both models for waves of very small or very large amplitude. However, for waves of intermediate amplitude there are important discrepancies between results.

2. A conventional Eulerian non-conservative model

The aim of this section is to present a well accepted Eulerian model for nonlinear elasticity. This system is of interest because of common usage in engineering sciences. The physical meaning of the various terms in the equations is also easy to examine. Moreover, this model can be extended to elastoplastic transformations, where the "plastic part" can be added in a standard way through a Maxwell type relaxation equation for the deviatoric part of the stress tensor. In the present paper, this model will be mainly used to:

- Highlight the issues present in such conventional modelling. These issues are related to the non-conservative character of the equations.
- Determine reference solutions, representative of the results obtained with engineering codes. In order to determine these reference solutions, a Riemann solver is built. These solutions will be compared in the forthcoming sections with the results of a conservative model formulated in terms of displacements.

The model presented in this section is somehow the reference at the engineering level [9,21]. It couples the nonlinear Euler system of compressible fluids with the system of linear elasticity for transverse waves. This system expresses mass, momentum and energy conservation laws augmented by evolution equations for the deviatoric part of the stress tensor:

$$\frac{\partial \rho}{\partial t} + \operatorname{div}(\rho \mathbf{v}) = 0,$$
$$\frac{\partial \rho \mathbf{v}}{\partial t} + \operatorname{div}(\rho \mathbf{v} \otimes \mathbf{v} + pI - S) = 0,$$
$$\frac{\partial \rho E}{\partial t} + \operatorname{div}((\rho E + p)\mathbf{v} - S\mathbf{v}) = 0,$$

$$\frac{D_J S}{Dt} + \frac{2}{3}\mu tr(V) I - 2\mu V = 0. \tag{1}$$

Here ρ, $\mathbf{v}$, and $E = \varepsilon + \varepsilon_e + \frac{1}{2}\mathbf{v}\cdot\mathbf{v}$ are, respectively, the density, the velocity vector and the total energy, $\varepsilon(\rho, p)$ is the internal energy verifying the Gibbs identity

$$T\mathrm{d}s = \mathrm{d}\varepsilon + p\mathrm{d}\left(\frac{1}{\rho}\right)$$

where T is the temperature and s is the entropy, $\varepsilon_e = \frac{S:S}{4\beta}$ is the elastic energy related to the shear stresses; $\beta = \rho\mu$, μ is the shear modulus, p is the thermodynamic pressure, and $S = (S_{ij})$ is the 3×3 symmetric traceless stress tensor. The rate of deformation tensor is given by

$$V = \frac{1}{2}\left(\frac{\partial \mathbf{v}}{\partial \mathbf{x}} + \left(\frac{\partial \mathbf{v}}{\partial \mathbf{x}}\right)^{\mathrm{T}}\right)$$

The notation $\frac{D_J S}{Dt}$ is the Jaumann derivative, and W is the spin tensor:

$$\frac{D_J S}{Dt} = \frac{DS}{Dt} + SW - WS, \quad W = \frac{1}{2}\left(\frac{\partial \mathbf{v}}{\partial \mathbf{x}} - \left(\frac{\partial \mathbf{v}}{\partial \mathbf{x}}\right)^{\mathrm{T}}\right),$$

where

$$\frac{D}{Dt} = \frac{\partial}{\partial t} + \mathbf{v}\cdot\nabla$$

is the material derivative. In particular, the Jaumann derivative coincides with the material derivative for potential flows. For small rotational deformations the Jaumann derivative can also be replaced by the material derivative. It is easy to obtain from (1) the evolution equation for entropy:

$$\rho\left(T\frac{Ds}{Dt} - \frac{S:S}{4\beta^2}\frac{D\beta}{Dt} + \frac{1}{4\beta}\frac{D(S:S)}{Dt}\right) - S:V = 0 \tag{2}$$

Taking into account that $tr(S) = 0$ and $tr(SB) = 0$ for $B = SW - WS$, we obtain from Eq. (2)

$$\frac{D(S:S)}{Dt} = 2\frac{DS}{Dt}:S = 2\frac{D_J S}{Dt}:S = -2\left(\frac{2}{3}\mu tr(V) I - 2\mu V\right):S = 4\mu(V:S) = 4\mu(S:V)$$

Finally, Eq. (2) will be reduced to:

$$\rho\left(T\frac{Ds}{Dt} - \frac{S:S}{4\beta^2}\frac{D\beta}{Dt}\right) = 0 \tag{3}$$

In absence of shock waves, elastic transformations are reversible and the model has to be isentropic. An extra evolution equation thus should be added in order to have an isentropic motion:

$$\frac{D\beta}{Dt} = 0 \tag{4}$$

Let us remark that [1] used a 1D variant of this model by making an assumption $\beta = \rho\mu = cte$ which is compatible with Eq. (4).

2.1. 1D system in presence of shear effects

In order to determine the Riemann problem solution, the flow model is examined in the 1D case (all variables depend only on (t, x)) in the presence of shear effects. To simplify the presentation, we will use the material derivative for the equations of the traceless stress tensor, and not the Jaumann derivatives. The system now reduces to:

$$
\begin{aligned}
&\frac{\partial \rho}{\partial t}+\frac{\partial \rho u}{\partial x}=0,\\
&\frac{\partial \rho u}{\partial t}+\frac{\partial \rho u^2+p-S_{11}}{\partial x}=0,\\
&\frac{\partial \rho v}{\partial t}+\frac{\partial \rho uv-S_{12}}{\partial x}=0,\\
&\frac{\partial \rho E}{\partial t}+\frac{\partial (\rho E+p-S_{11})u-S_{12}v}{\partial x}=0,\\
&\frac{\partial \rho S_{11}}{\partial t}+\frac{\partial \rho S_{11}u}{\partial x}=\frac{4}{3}\beta\frac{\partial u}{\partial x},\quad \beta=\rho\mu,\\
&\frac{\partial \rho S_{22}}{\partial t}+\frac{\partial \rho S_{22}u}{\partial x}=-\frac{2}{3}\beta\frac{\partial u}{\partial x},\\
&\frac{\partial \rho S_{12}}{\partial t}+\frac{\partial \rho S_{12}u}{\partial x}=\beta\frac{\partial v}{\partial x},\\
&\frac{D\beta}{Dt}=0.
\end{aligned}
\tag{5}
$$

The first four equations are conventional equations of continuum mechanics. The total specific energy E contains internal, elastic and kinetic energy. The other equations correspond to the evolution of the traceless stress tensor. These equations are obtained on the basis of Hooke law in the limit of small deformations. Under compression $\frac{\partial u}{\partial x}\leqslant 0$, a negative stress S_{11} and a positive stress S_{22} are created. Their contribution augments the resistance to compression in the x-direction. Under shear deformation $\frac{\partial v}{\partial x}\neq 0$, stress S_{12} is created and augments the resistance to shear.

Model (5) will be used to determine reference solutions which will be studied in the next section.

2.2. Simple waves

System (5) can be written in quasi-linear form:

$$
\frac{\partial \mathbf{W}}{\partial t}+A(\mathbf{W})\frac{\partial \mathbf{W}}{\partial x}=0,
\tag{6}
$$

where

$$
\mathbf{W}=\begin{pmatrix}\rho\\ u\\ p\\ S_{11}\\ S_{22}\\ \mu\\ v\\ S_{12}\end{pmatrix},\quad
A(\mathbf{W})=\begin{pmatrix}
u & \rho & 0 & 0 & 0 & 0 & 0 & 0\\
0 & u & \frac{1}{\rho} & -\frac{1}{\rho} & 0 & 0 & 0 & 0\\
0 & \rho c^2 & u & 0 & 0 & 0 & 0 & 0\\
0 & -\frac{4}{3}\mu & 0 & u & 0 & 0 & 0 & 0\\
0 & \frac{2}{3}\mu & 0 & 0 & u & 0 & 0 & 0\\
0 & -\mu & 0 & 0 & 0 & u & 0 & 0\\
0 & 0 & 0 & 0 & 0 & 0 & u & -\frac{1}{\rho}\\
0 & 0 & 0 & 0 & 0 & 0 & -\mu & u
\end{pmatrix}.
$$

The system is hyperbolic with characteristic speeds given by: u, $u\pm\sqrt{\frac{\mu}{\rho}}$ and $u\pm\sqrt{c^2+\frac{4}{3}\frac{\mu}{\rho}}$. The contact characteristic $\frac{dx}{dt}=u$ is of multiplicity four. Here c is the thermodynamic sound speed. Standard calculations show that the characteristic fields u and $u\pm\sqrt{\frac{\mu}{\rho}}$ are linearly degenerate while $u\pm\sqrt{c^2+\frac{4}{3}\frac{\mu}{\rho}}$ is a genuinely nonlinear field.

The structure of the matrix $A(\mathbf{W})$ allows a splitting of the system into two subsystems:

- a subsystem involving acoustic and contact waves propagating with speeds $u\pm\sqrt{c^2+\frac{4}{3}\frac{\mu}{\rho}}$ and u,
- a subsystem describing shear waves propagating with speeds $u\pm\sqrt{\frac{\mu}{\rho}}$.

We examine self-similar solutions of (6):

$$\mathbf{W} = \mathbf{W}(\xi), \quad \xi = x/t.$$

The system (6) becomes

$$(A - \xi I)\frac{\mathrm{d}\mathbf{W}}{\mathrm{d}\xi} = 0 \tag{7}$$

It follows from here that ξ is an eigenvalue of the matrix A, and $\frac{\mathrm{d}\mathbf{W}}{\mathrm{d}\xi}$ is the corresponding right eigenvector of A. We consider now separately three types of waves.

2.2.1. Acoustic wave

The subsystem composed of the first 6 equations is considered. If

$$\xi = u \mp \sqrt{c^2 + \frac{4}{3}\frac{\mu}{\rho}}$$

the following relations are hold:

$$\pm\sqrt{c^2 + \frac{4}{3}\frac{\mu}{\rho}}\mathrm{d}\rho + \rho\mathrm{d}u = 0,$$

$$\pm\sqrt{c^2 + \frac{4}{3}\frac{\mu}{\rho}}\mathrm{d}u + \frac{1}{\rho}\mathrm{d}(p - S_{11}) = 0,$$

$$\pm\sqrt{c^2 + \frac{4}{3}\frac{\mu}{\rho}}\mathrm{d}p + \rho c^2\mathrm{d}u = 0,$$

$$\pm\sqrt{c^2 + \frac{4}{3}\frac{\mu}{\rho}}\mathrm{d}S_{11} - \frac{4}{3}\mu\mathrm{d}u = 0,$$

$$\mathrm{d}(2S_{22} + S_{11}) = 0, \quad \mathrm{d}\beta = 0.$$

It follows from here that:

$$\begin{aligned}
&\mathrm{d}p = c^2\,\mathrm{d}\rho, \quad \mathrm{d}\beta = 0,\\
&\mathrm{d}u = \mp\frac{1}{\rho c^2}\sqrt{c^2 + \frac{4}{3}\frac{\beta}{\rho^2}}\mathrm{d}p\\
&\frac{1}{\rho^2 c^2}\,\mathrm{d}p + \frac{3}{4\beta}\,\mathrm{d}S_{11} = 0
\end{aligned} \tag{8}$$

It is now necessary to specify the equation of state (EOS). For the sake of simplicity we consider the stiffened gas EOS:

$$\varepsilon = \frac{p + \gamma p_\infty}{(\gamma - 1)\rho} \tag{9}$$

The sound speed is defined by:

$$c^2 = \gamma\frac{p + p_\infty}{\rho}$$

By integrating system (8) between initial state with subscript 0 and final state with superscript *, we have:

$$\frac{p^* + p_\infty}{\rho^{*\gamma}} = \frac{p_0 + p_\infty}{\rho_0^\gamma}, \tag{10}$$

$$u^* = u_0 \mp \frac{1}{\gamma}\int_{p_0+p_\infty}^{p^*+p_\infty}\sqrt{\frac{\gamma\tilde{p}^{-\frac{\gamma+1}{\gamma}}}{K_0} + \frac{4\beta}{3\gamma K_0^2}\tilde{p}^{-\frac{2(\gamma+1)}{\gamma}}}\,\mathrm{d}\tilde{p}, \quad K_0 = \frac{\rho_0}{(p_0 + p_\infty)^{\frac{1}{\gamma}}}, \tag{11}$$

$$(p^* + p_\infty)^{-\frac{1}{\gamma}} - (p_0 + p_\infty)^{-\frac{1}{\gamma}} - K_0\frac{3}{4\beta}\left(S_{11}^* - S_{110}\right) = 0. \tag{12}$$

This system provides three relations through rarefaction waves. The negative (positive) sign in the expression for Riemann invariants (11) corresponds to a left-facing (right-facing) wave. The tangential velocity v and the component S_{12} do not vary in such a wave:

$$\mathrm{d}v = 0, \quad \mathrm{d}S_{12} = 0.$$

2.2.2. Shear waves

We now consider the subsystem formed by the last two equations of system (6). For

$$\xi = u \pm \sqrt{\frac{\mu}{\rho}}$$

the following relations are verified:

$$\mathrm{d}\left(S_{12} \mp \sqrt{\beta} v\right) = 0 \tag{13}$$

By integrating Eq. (13) between initial state with subscript 0 and final state with superscript *, we have the following Riemann invariant:

$$\sqrt{\beta}(v_0 \mp v^*) = S_{120} \mp S_{12}^* \tag{14}$$

In expression Eq. (14) for Riemann invariants, a negative (positive) sign corresponds to the right-facing (left-facing) wave.

2.2.3. Contact wave

For contact characteristics $\boldsymbol{\xi} = u$ system (7) becomes:

$$\mathrm{d}u = 0,$$
$$\mathrm{d}(p - S_{11}) = 0,$$
$$\mathrm{d}(S_{12}) = 0,$$
$$\mathrm{d}(v) = 0.$$

These relations express the continuity of the velocity vector, generalized pressure and shear stress component through the contact characteristics.

2.3. Shock relations

Conventional shock relations are not available for system (5) because it cannot be written in divergence form. This poses serious difficulties for the Riemann problem solution and its numerical approximation with finite difference, finite volume or finite element methods. It is the reason why a conservative formulation will be developed in a forthcoming section.

As we have seen before the model needs an additional equation to be isentropic:

$$\frac{D\beta}{Dt} = 0.$$

Combining that equation with the mass conservation, we have:

$$\frac{\partial \rho\beta}{\partial t} + \frac{\partial \rho u\beta}{\partial x} = 0.$$

From which we deduce the jump relation: $\beta^* = \beta_0$. This equation was also used by [1] who supposed $\beta = \beta_0$ in the entire domain.

The first four equations of system (5) are in conservative form and thus the Rankine–Hugoniot relations between pre-and post-shock states are:

$$\mathbf{F}^* - D\mathbf{U}^* = \mathbf{F}_0 - D\mathbf{U}_0 \tag{15}$$

where D is the shock speed, and the vectors of conservative variables and flux are given by:

$$\mathbf{U} = (\,\rho \quad \rho u \quad \rho v \quad \rho E\,)^{\mathrm{T}},$$
$$\mathbf{F} = \big(\,\rho u \quad \rho u^2 + p - S_{11} \quad \rho uv - S_{12} \quad (\rho E + p - S_{11})u - vS_{12}\,\big)^{\mathrm{T}}.$$

The next three equations of system (5) are in non-conservative form. However, we can rewrite non-conservative terms in the form

$$\beta\frac{\partial u}{\partial x} = \frac{\partial(\beta u)}{\partial x} - u\frac{\partial \beta}{\partial x},$$
$$\beta\frac{\partial v}{\partial x} = \frac{\partial(\beta v)}{\partial x} - v\frac{\partial \beta}{\partial x}.$$

At shocks β is continuous. If, moreover, it is a function with bounded derivatives, the non-conservative product which appeared now is a locally integrable function. Hence, the following Rankine–Hugoniot relations can be obtained:

$$\begin{aligned}
&\rho^* S^*_{11}(u^* - D) - \frac{4}{3}\beta^* u^* = \rho_0 S_{110}(u_0 - D) - \frac{4}{3}\beta_0 u_0\\
&\rho^* S^*_{22}(u^* - D) + \frac{2}{3}\beta^* u^* = \rho_0 S_{220}(u_0 - D) + \frac{2}{3}\beta_0 u_0\\
&\rho^* S^*_{12}(u^* - D) - \beta^* v^* = \rho_0 S_{110}(u_0 - D) - \beta_0 v_0
\end{aligned} \tag{16}$$

A more suitable form of system (15) and (16) can be obtained:

$$e^* - e_0 + \left(\frac{p^* + p_0}{2}\right)\left(\frac{1}{\rho^*} - \frac{1}{\rho_0}\right) = 0 \tag{17}$$

$$S_{110} - S^*_{11} = \frac{4}{3}\frac{\beta}{m}(u_0 - u^*) \tag{18}$$

$$m^2 = \frac{(p_0 - p^*)}{\left(\frac{1}{\rho^*} - \frac{1}{\rho_0}\right)} + \frac{4}{3}\beta \tag{19}$$

$$u^* = u_0 \pm \sqrt{\frac{p_0 - p^*}{\left(\frac{1}{\rho^*} - \frac{1}{\rho_0}\right)} + \frac{4}{3}\beta\left(\frac{1}{\rho^*} - \frac{1}{\rho_0}\right)} \tag{20}$$

$$v^* = v_0 \tag{21}$$

$$S^*_{12} = S_{120} \tag{22}$$

$$S_{220} - S^*_{22} = -\frac{2}{3}\frac{\beta}{m}(u_0 - u^*) \tag{23}$$

Here $m = \rho_{\mathrm{R}}(u_{\mathrm{R}} - D) = \rho^*_{\mathrm{R}}(u^*_{\mathrm{R}} - D)$ is the mass flow rate across the shock front. We consider again the material governed by the stiffened gas EOS. With this EOS it is possible to determine from (17) to (19) the density along the Hugoniot curve and the shock mass flow rate as a function of pressure in the post-shock state:

$$\rho^* = \rho_0\frac{(\gamma+1)(p^* + p_\infty) + (\gamma-1)(p_0 + p_\infty)}{(\gamma-1)(p^* + p_\infty) + (\gamma+1)(p_0 + p_\infty)} \tag{24}$$

$$m^2 = \frac{\rho_0((\gamma+1)(p^* + p_\infty) + (\gamma-1)(p_0 + p_\infty))}{2} + \frac{4}{3}\beta \tag{25}$$

It is worth to mention that Eq. (20) has not a unique solution for a given velocity difference. By noting $\Phi = \frac{p^* + p_\infty}{p_0 + p_\infty}$ Eq. (20) becomes:

$$\Phi^3 + a\Phi^2 + b\Phi + c = 0 \tag{26}$$

with

$$a = -(\gamma+1)\frac{\rho_R}{2(p_0+p_\infty)}(u^*-u_0)^2 - 2 + \frac{1}{(\gamma+1)}\left((\gamma-1)+\frac{8}{3}\frac{\beta}{\rho_0(p_0+p_\infty)}\right),$$

$$b = -2(1-\gamma)\frac{\rho_0}{2(p_0+p_\infty)}(u^*-u_0)^2 + 1 - \frac{2}{(\gamma+1)}\left((\gamma-1)+\frac{8}{3}\frac{\beta}{\rho_0(p_0+p_\infty)}\right)$$

$$c = \frac{\left(-(\gamma-1)^2\frac{\rho_0}{2(p_0+p_\infty)}(u^*-u_0)^2 + (\gamma-1) + \frac{8}{3}\frac{\beta}{\rho_0(p_0+p_\infty)}\right)}{(\gamma+1)}.$$

For a given velocity in the post-shock state u^*, the physical solution corresponds to $\Phi \geqslant 1$. With this condition, Eq. (26) has a unique solution. Once this equation is solved, the entire shock state is determined with (18), (21)–(25).

All relations are now available for the Riemann problem solution.

2.4. Riemann problem

The Riemann problem involves five waves and four principal wave patterns as shown in Fig. 1 (vacuum appearance is not considered here). With the previous relations it is possible to determine the states between the waves. An iterative solver is used. The iteration variable is the contact wave velocity u^*. The iterations are done with the Newton–Raphson method. The initial condition for the iterative method reads:

$$u^* = \frac{(p_L - S_{11L}) - (p_R - S_{11R}) + Z_R u_R + Z_L u_L}{Z_R + Z_L}, \quad Z = \rho\left(c^2 + \frac{4}{3}\frac{\mu}{\rho}\right)$$

Then we have to consider the four cases summarized in Fig. 1.

If $u^* > u_R$, we use the shock relations (15) and (16) on the right. Eq. (26) is solved and the pressure behind the shock p^* is determined. Then Eqs. (18), (23)–(25) are solved to determine the other variables.

If $u^* \leqslant u_R$ we use rarefaction wave Eqs. (10)–(12) on the right. Eq. (11) needs iterative resolution.

The same procedure is used for the left-facing wave. The two shear waves corresponding to the characteristics $u \pm \sqrt{\frac{\mu}{\rho}}$ have not to be considered for the determination of contact wave velocity and normal stress.

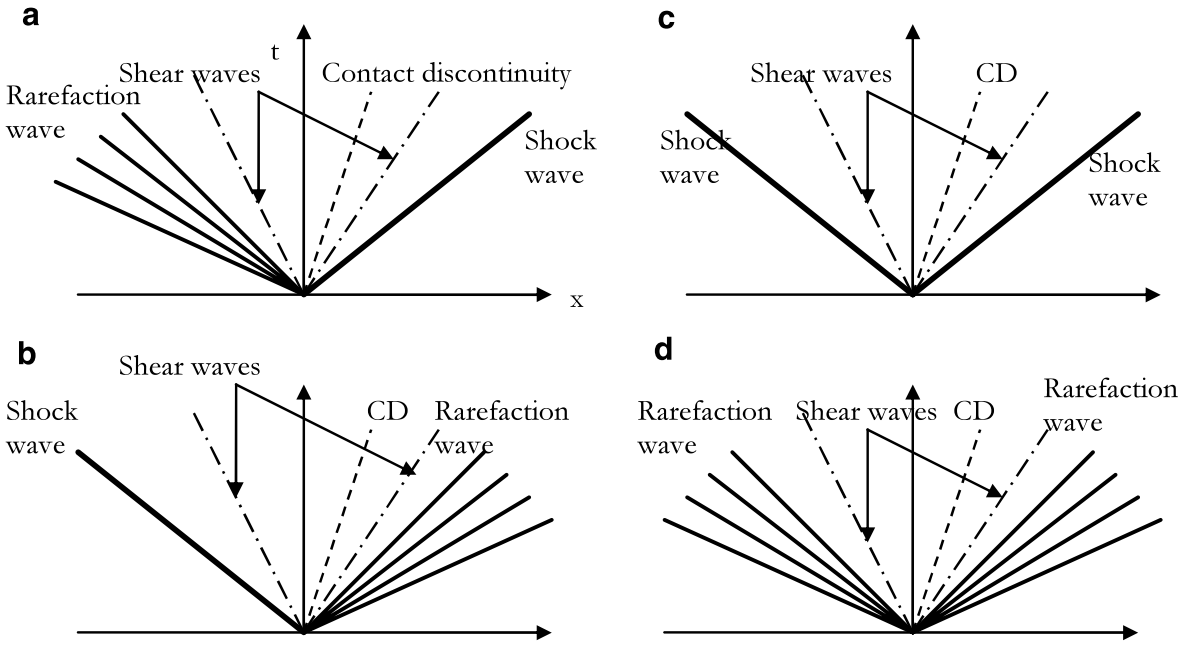

Fig. 1. The four possible Riemann problem wave patterns for the compressible elastic flow model.

Once normal stress is determined on both sides it is then necessary to examine the difference $h(u^*) = (p - S_{11})^*_{\mathrm{R}} - (p - S_{11})^*_{\mathrm{L}}$. If $| h(u^*) | < \delta$ (for some small δ), a new value of u^* (denoted by $\tilde{u}^*$) is determined by Newton–Raphson method:

$$\tilde{u}^* = u^* - \frac{\left(p^*_{\mathrm{L}} - S^*_{11\mathrm{L}}\right) - \left(p^*_{\mathrm{R}} - S^*_{11\mathrm{R}}\right)}{\frac{\mathrm{d}\left(p^*_{\mathrm{L}} - S^*_{11\mathrm{L}}\right)}{\mathrm{d}u} - \frac{\mathrm{d}\left(p^*_{\mathrm{R}} - S^*_{11\mathrm{R}}\right)}{\mathrm{d}u}}$$

When convergence is reached, the remaining variables of states $\mathbf{U}^*_{\mathrm{R}}$ and $\mathbf{U}^*_{\mathrm{L}}$ are determined by shock relations (26), (24), (25), (18), (23) or by Riemann invariants (10)–(12) (except the tangential velocity and stress). The last variables are determined with the help of relations (14). Their combination results in:

$$S^*_{12} = \frac{S_{12\mathrm{R}} + S_{12\mathrm{L}} + \sqrt{\beta}(v_{\mathrm{R}} - v_{\mathrm{L}})}{2},$$

$$v^* = \frac{\sqrt{\beta}v_{\mathrm{L}} + \sqrt{\beta}v_{\mathrm{R}} + S_{12\mathrm{R}} - S_{12\mathrm{L}}}{2\sqrt{\beta}}.$$

2.5. Reference results

In this section, we present different test problems that will be used to compare the models. In all computations the material EOS parameters are taken equal to: $p_\infty = 6 \times 10^8$ Pa, $\gamma = 4.4$.

2.5.1. Fluid limit

In this example the shear modulus μ is set to zero. The model thus reduces to the Euler equations of compressible fluids. We consider a shock tube where initially an interface separates the material at rest with high pressure $p = 10^{10}$ Pa and density $\rho = 1000$ kg/m^3 on the left, and the same material at rest with pressure $p = 10^5$ Pa and density $\rho = 1000$ kg/m^3 on the right. The interface is initially located at $x_i = 0.5$ m. Fig. 2 shows computed results at time $t = 50$ μs. Symbols correspond to the exact solution with the present elastic flow model, and lines to the exact solution of the Euler equations. The results are in perfect agreement with both methods.

2.5.2. Elastic shock tube

We consider a shock tube where an interface separates initially the elastic material with high pressure $p = 10^{10}$ Pa and density $\rho = 7800$ kg/m^3 on the left, and the same material at rest with pressure $p = 10^5$ Pa and density $\rho = 7800$ kg/m^3 on the right. In both materials, we took $\beta = 10^{14}$ Pa kg/m^3. A tangential velocity discontinuity is imposed: $v = -100$ m/s on the left, and $v = 100$ m/s on the right. The interface is initially located at $x_i = 0.6$ m. Fig. 3 shows computed results at time $t = 150$ μs. We can see five waves: a rarefaction wave on the left, a shock wave on the right, two waves corresponding to the shear waves and the contact discontinuity. Results of Fig. 3 will be considered as reference results and will be used for comparison with a more sophisticated conservative flow model developed in the next section (See Fig. 4).

3. Conservative Eulerian model of nonlinear elasticity

The hyperbolic conservative model presented below was developed by [5,10]. Some modifications are made concerning a more suitable form of governing equations. They form a set of evolution equations for a local cobasis. Also, the equation of state is given in terms of the invariants of the Almansi deformation tensor in a form which separates hydrodynamic and shear effects. The essential difference with respect to the model considered in Section 2 is that the evolution equations are formulated in terms of displacements, and not in terms of stresses. The advantage of this approach is that the governing equations are naturally objective, there is no need to add Jaumann type derivatives, only material derivatives are present.

3.1. Basic definitions

We will formulate the model in 3D case. Let $\mathbf{X} = (X^\alpha)$ be the Lagrangian coordinates, $\alpha = 1, 2, 3$, $\mathbf{x} = (x^i)$ be the Eulerian coordinates, $i = 1, 2, 3$. We define the deformation gradient

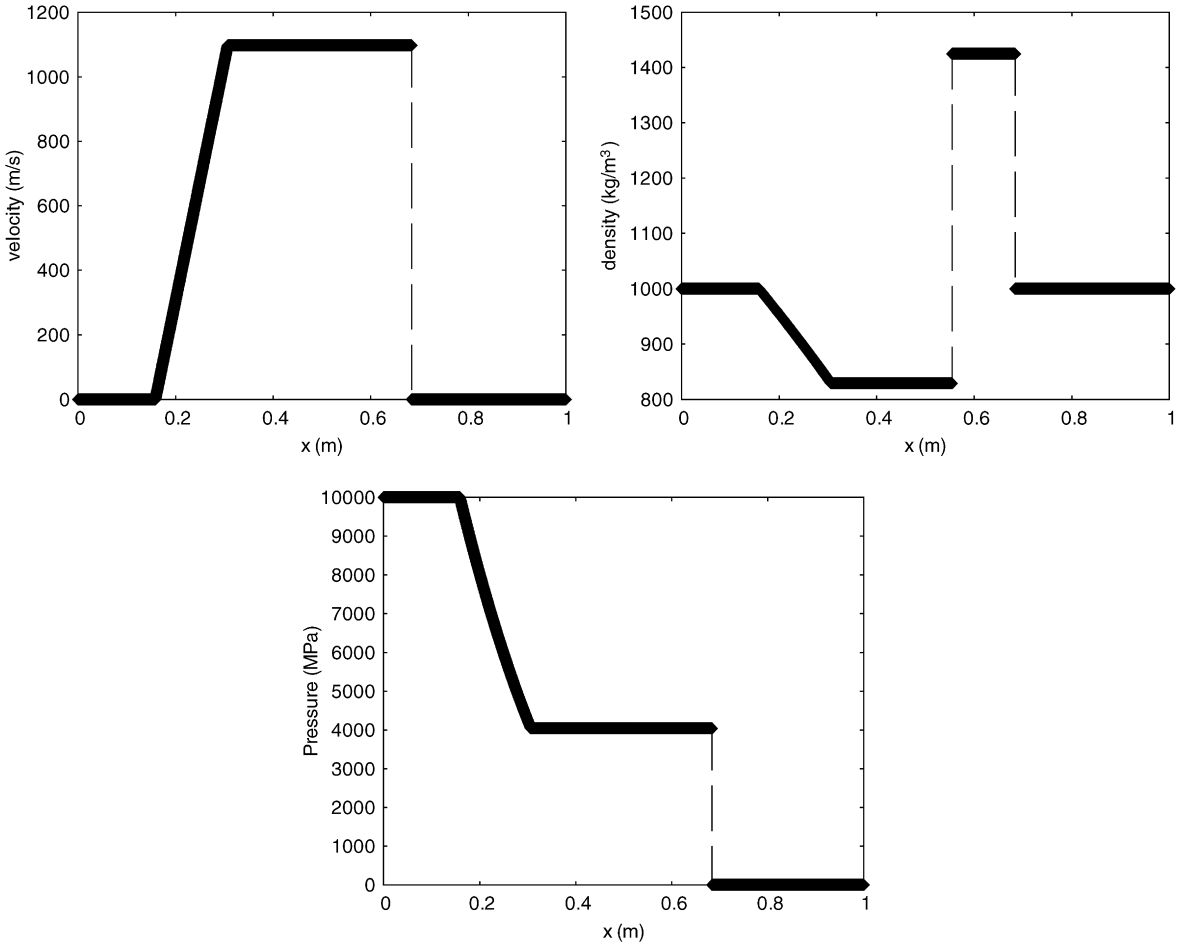

Fig. 2. Shock tube test problem in the fluid limit. The "exact" solution of the elastic model (symbols) and exact solution of Euler equations (lines) are shown at time $t = 50$ μs. The agreement is perfect.

$$F = \frac{\partial \mathbf{x}}{\partial \mathbf{X}},$$

Usually, conservative elasticity models use the right Cauchy–Green tensor (dilatation tensor)

$$C^{\mathrm{R}} = F^{\mathrm{T}}F$$

However, in our approach we will use the inverse of left Cauchy–Green tensor $C^{\mathrm{L}} = FF^{\mathrm{T}}$ which will be denoted by G

$$G = (C^{\mathrm{L}})^{-1} = (F^{\mathrm{T}})^{-1}F^{-1}$$

The tensor G is more convenient for the Eulerian formulation of governing equations of isotropic elastic materials. In particular, it determines the Almansi deformation tensor (Eulerian deformation tensor):

$$\mathcal{A} = \frac{I - G}{2}$$

We introduce the *curvilinear cobasis (covectors)*

$$\mathbf{e}^{\alpha} = \nabla X^{\alpha}, \quad \alpha = 1, 2, 3$$

which is dual to the natural *curvilinear basis*

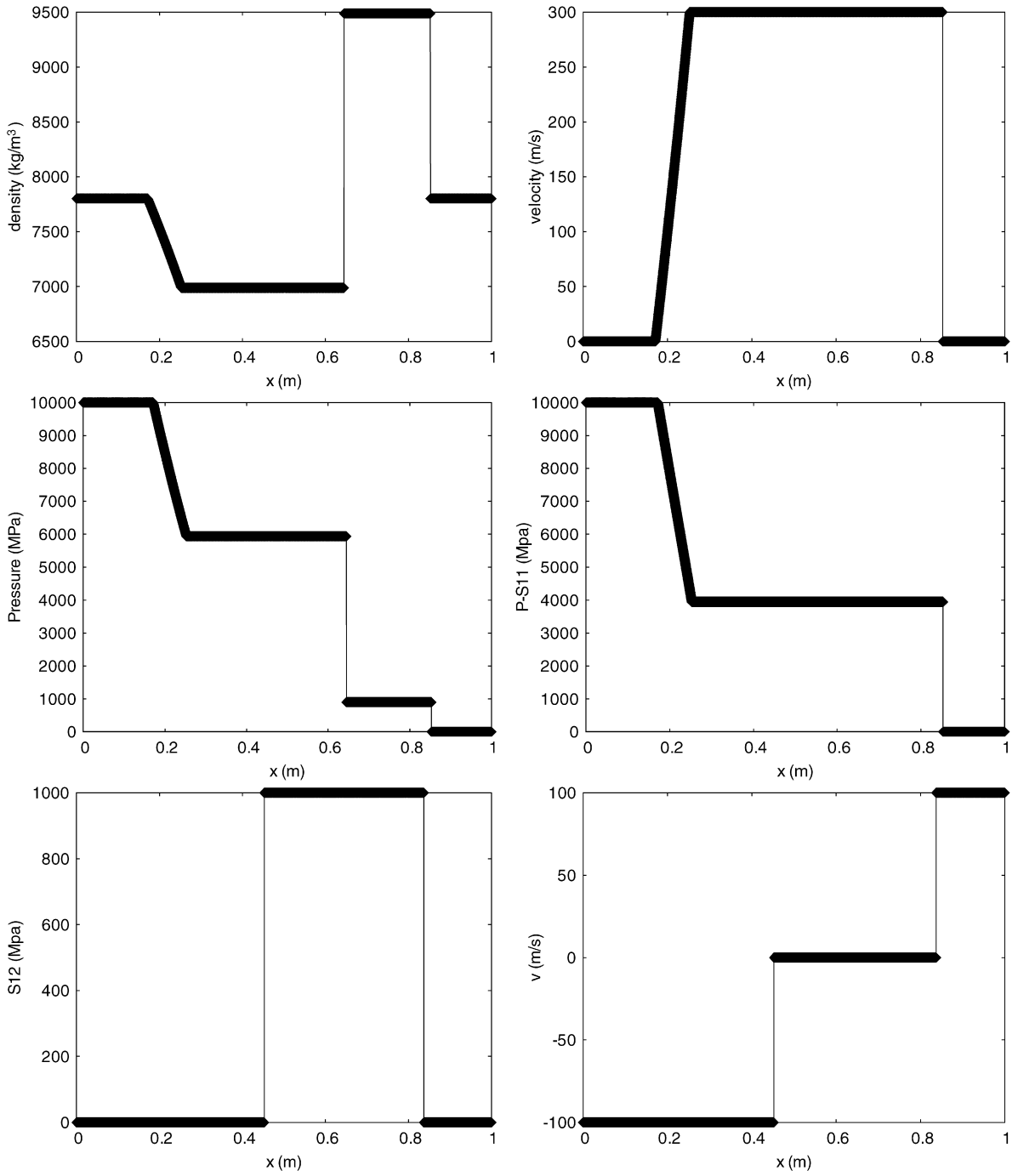

Fig. 3. Elastic shock tube test problem. The material is considered here as elastic in the presence of an initial tangential velocity discontinuity. Solution is shown at time $t = 150$ μs. Five waves are visible propagating with different velocities: three classical waves (rarefaction on the left, shock wave on the right and the contact discontinuity), and two shear waves.

$$\mathbf{e}_\alpha = \frac{\partial \mathbf{x}}{\partial X^\alpha}, \quad \alpha = 1, 2, 3$$

In particular, the vector $\mathbf{e}^\alpha$ is the α-th column of $(F^{-1})^{\mathrm{T}}$:

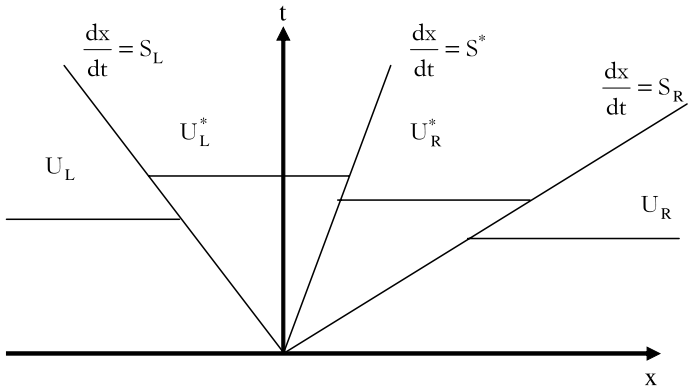

Fig. 4. HLLC approximate solver. Solution in the star region consists of two constant states separated from each other by a middle wave of speed S^*

$$(F^{-1})^{\mathrm{T}} = \begin{pmatrix} \frac{\partial X^1}{\partial x^1} & \frac{\partial X^2}{\partial x^1} & \frac{\partial X^3}{\partial x^1} \\ \frac{\partial X^1}{\partial x^2} & \frac{\partial X^2}{\partial x^2} & \frac{\partial X^3}{\partial x^2} \\ \frac{\partial X^1}{\partial x^3} & \frac{\partial X^2}{\partial x^3} & \frac{\partial X^3}{\partial x3} \end{pmatrix} = \begin{pmatrix} \mathbf{e}^1 & \mathbf{e}^2 & \mathbf{e}^3 \end{pmatrix} = \begin{pmatrix} e_1^1 & e_1^2 & e_1^3 \\ e_2^1 & e_2^2 & e_2^3 \\ e_3^1 & e_3^2 & e_3^3 \end{pmatrix}, \quad \mathfrak{e}_j^\alpha = (\mathbf{e}^\alpha)_j = \frac{\partial X^\alpha}{\partial x^j}.$$

The scalar product of these vectors satisfies

$$\mathbf{e}_\alpha \cdot \mathbf{e}^\beta = \delta_\alpha^\beta$$

where δ_α^β are the Kronecker symbols. With these definitions

$$G = \sum_{\alpha=1}^{3} \mathbf{e}^\alpha \otimes \mathbf{e}^\alpha, \quad G^{-1} = \sum_{\alpha=1}^{3} \mathbf{e}_\alpha \otimes \mathbf{e}_\alpha. \tag{27}$$

Here for any vectors $\mathbf{a}$ and $\mathbf{b}$ the matrix of the tensor product $\mathbf{a} \otimes \mathbf{b}$ is defined as follows

$$(\mathbf{a} \otimes \mathbf{b})_j^i = a^i b_j,$$

(i are lines and j are columns). Since

$$\frac{DX^\alpha}{Dt} = 0$$

we have by taking the gradient of that equation:

$$\frac{\partial \mathbf{e}^\alpha}{\partial t} + \nabla(\mathbf{v} \cdot \mathbf{e}^\alpha) = 0, \quad \mathrm{rot}\, \mathbf{e}^\alpha = 0 \tag{28}$$

In particular, Eqs. (27) and (28) imply that

$$\frac{DG}{Dt} + G\frac{\partial \mathbf{v}}{\partial \mathbf{x}} + \left(\frac{\partial \mathbf{v}}{\partial \mathbf{x}}\right)^{\mathrm{T}} G = 0$$

It is interesting to note that the left hand side of this equation can be considered as objective derivative.

Remark 1. The differential constraint in Eq. (28) $\mathrm{rot}\, \mathbf{e}^\alpha = 0$ is compatible with the evolution equation for $\mathbf{e}^\alpha$: if $\mathrm{rot}\, \mathbf{e}^\alpha = 0$ vanishes at time $t = 0$, it vanishes at all $t > 0$. This constraint is automatically satisfied in 1D case. However, in multidimensional settings a proper handling is necessary because, numerically, differences arise. Actually, the best strategy for solving such a problem was proposed by [10,11] who considered an augmented system of hyperelasticity where the evolution equation for $\mathrm{rot}((F^{-1})^{\mathrm{T}})$ has been added. The columns of $\mathrm{rot}((F^{-1})^{\mathrm{T}})$ are the vectors $\mathbf{w}^\alpha = \mathrm{rot}\, \mathbf{e}^\alpha$. The evolution Eq. (28) was replaced in [10] by:

$$\frac{\partial \mathbf{e}^\alpha}{\partial t} + \nabla(\mathbf{v} \cdot \mathbf{e}^\alpha) = -\mathrm{rot}\mathbf{e}^\alpha \wedge \mathbf{v}. \tag{29}$$

The "geometric Eq. (29) is equivalent to Miller and Colella' one (2001) written for $\mathrm{rot}((F^{-1})^T)$ (see Eq. (9) in [10] where the notation g was used for the matrix F^{-1}). For the vectors $\mathbf{w}^\alpha = \mathrm{rot}\mathbf{e}^\alpha$ the following conservative system can be obtained from (29):

$$\frac{\partial \mathbf{w}^\alpha}{\partial t} + \mathrm{rot}\,(\mathbf{w}^\alpha \wedge \mathbf{v}) = 0.$$

Since

$$\mathrm{rot}\,(\mathbf{w}^\alpha \wedge \mathbf{v}) = \mathbf{w}^\alpha \mathrm{div}\,\mathbf{v} - \mathbf{v}\mathrm{div}\,\mathbf{w}^\alpha + \frac{\partial \mathbf{w}^\alpha}{\partial \mathbf{x}}\mathbf{v} - \frac{\partial \mathbf{v}}{\partial \mathbf{x}}\mathbf{w}^\alpha,$$

it is equivalent to the following equation

$$\frac{\partial \mathbf{w}^\alpha}{\partial t} + \mathrm{div}(\mathbf{v}\otimes\mathbf{w}^\alpha - \mathbf{w}^\alpha \otimes \mathbf{v}) = 0. \tag{30}$$

The divergence of a second-order tensor is a vector; its components are the divergence of each column of the tensor. To interpret the geometry of deformation, it is convenient to use the local cobasis vectors $\mathbf{e}^\alpha$ as unknown variables. In cartesian coordinates Eqs. (29) and (30) are

$$\frac{\partial \mathrm{e}_j^\alpha}{\partial t} + \frac{\partial}{\partial x^j}\left(\sum_{i=1}^{3} \mathrm{e}_i^\alpha v_i\right) = (\mathbf{v}\wedge\mathbf{w}^\alpha)_j,$$

$$\frac{\partial w_j^\alpha}{\partial t} + \sum_{i=1}^{3}\frac{\partial}{\partial x^i}\left(v_i w_j^\alpha - v_j w_i^\alpha\right) = 0.$$

A numerical strategy that control the gauge constraint $\mathbf{w}^\alpha = 0$ was developed in [10,11]. In our study we will concentrate only on the 1D problems.

3.2. Isotropic elastic body

Let e be the specific internal energy,

$$e = e(G, s)$$

where s is the specific entropy. Let Ω_0 be a domain in the reference configuration, and Ω its image in the actual configuration. Let us consider the variation of the internal energy $\mathcal{E}_i$ at fixed value of s:

$$\delta\mathcal{E}_i = \delta\int_\Omega \rho e(G,s)\mathrm{d}\Omega$$

We have

$$\delta\mathcal{E}_i = \delta\int_\Omega \rho e(G,s)\,\mathrm{d}\Omega = \int_{\Omega_0}\rho_0\delta e(G,s)\,\mathrm{d}\Omega_0 = \int_{\Omega_0}\rho_0 tr\left(\frac{\partial e}{\partial G}\delta G\right)\mathrm{d}\Omega_0$$

The matrix

$$\frac{\partial e}{\partial G}$$

is symmetric. Let $\delta\mathbf{x}$ be the variation of the particle positions at the actual configuration considered as a function of Lagrangian coordinates [5,14]. Since

$$\delta G = (\delta F^{-1})^{\mathrm{T}}F^{-1} + (F^{-1})^{\mathrm{T}}\delta F^{-1} = -(F^{-1}\delta F F^{-1})^{\mathrm{T}}F^{-1} - (F^{-1})^{\mathrm{T}}F^{-1}\delta F F^{-1} = -\left(\frac{\partial\delta\mathbf{x}}{\partial\mathbf{x}}\right)^{\mathrm{T}}G - G\frac{\partial\delta\mathbf{x}}{\partial\mathbf{x}}$$

we obtain

$$\delta\mathcal{E}_i = -\int_{\Omega_0} 2\rho_0 tr\left(\frac{\partial e}{\partial G}G\frac{\partial\delta\mathbf{x}}{\partial\mathbf{x}}\right)\mathrm{d}\Omega_0 = -\int_\Omega 2\rho tr\left(\frac{\partial e}{\partial G}G\frac{\partial\delta\mathbf{x}}{\partial\mathbf{x}}\right)\mathrm{d}\Omega = \int_\Omega tr\left(\sigma\frac{\partial\delta\mathbf{x}}{\partial\mathbf{x}}\right)\mathrm{d}\Omega$$

The tensor

$$\sigma = -2\rho\frac{\partial e}{\partial G}G$$

is the *Murnaghan stress tensor* (see [5,6]. It is symmetric, if e is isotropic function. Indeed, in the isotropic case, e depends only on the invariants of G which can be defined as

$$J_i = tr(G^i), \quad i = 1,2,3$$

In particular, the determinant of G (denoted by $\mid G \mid$) can be expressed in terms of J_i in the form

$$\mid G \mid = \frac{2J_3 - 3J_1J_2 + J_1^3}{6}$$

It can be proved that (see, for example, [4])

$$\frac{\partial \mid G \mid}{\partial G} = \mid G \mid G^{-1}, \quad \frac{\partial J_i}{\partial G} = iG^{i-1}, \quad i = 1,2,3$$

Hence

$$\sigma = -2\rho\frac{\partial e}{\partial G}G = -2\rho\left(\frac{\partial e}{\partial J_1}I + 2\frac{\partial e}{\partial J_2}G + 3\frac{\partial e}{\partial J_3}G^2\right)G = -2\rho G\frac{\partial e}{\partial G} = \sigma^{\mathrm{T}}$$

Here the density ρ is expressed by

$$\rho = \rho_0 \mid G \mid^{1/2}$$

3.2.1. EOS formulation in separate form

It is natural to present the energy in the form which is combination of a "hydrodynamic" part and an "elastic" part:

$$e = \varepsilon(\rho, s) + \varepsilon_e(g, s)$$

where

$$g = \frac{G}{\mid G \mid^{1/3}}.$$

The hydrodynamic part of the energy $\varepsilon(\rho, s)$ can be taken in the form of stiffened gas EOS:

$$\varepsilon(\rho, p) = \frac{p + \gamma p_\infty}{\rho(\gamma - 1)}, \quad p + p_\infty = \exp\left(\frac{s - s_0}{c_v}\right)\rho^\gamma, \quad s_0 = \text{const.} \tag{31}$$

Here γ is the polytropic exponent, p_∞ is a constant, c_v is the specific heat at constant volume.

The elastic part of the internal energy $\varepsilon_e(g, s)$ depends on the tensor g. The tensor g has a unit determinant, so it is unaffected by the volume change. This idea to take the arguments of the internal energy in the form ρ, g and s was first proposed by [7] (see also [13]), but for the dependence of the energy on the right Cauchy–Green tensor. The simplest example of the elastic energy is

$$\varepsilon_e(g, s) = \frac{\mu(s)}{4\rho_0}tr((g - I)^2) = \frac{\mu(s)}{4\rho_0}\left(\frac{J_2}{\mid G \mid^{2/3}} - \frac{2J_1}{\mid G \mid^{1/3}} + 3\right) \tag{32}$$

where $\mu(s)$ is the shear modulus which can depend on the entropy. The stress tensor will be then

$$\begin{aligned}\sigma &= -2\rho\frac{\partial e}{\partial G}G = -\rho^2\frac{\partial \varepsilon}{\partial \rho}I - 2\rho G\frac{\mu(s)}{4\rho_0}\left(\frac{2G}{\mid G \mid^{2/3}} - \frac{2}{3}\frac{J_2}{\mid G \mid^{1+2/3}} \mid G \mid G^{-1} - \frac{2I}{\mid G \mid^{1/3}} + \frac{2J_1}{3 \mid G \mid^{1+1/3}} \mid G \mid G^{-1}\right) \\ &= -pI - \mu(s)\frac{\rho}{\rho_0}\left(\frac{1}{\mid G \mid^{2/3}}\left(G^2 - \frac{J_2}{3}I\right) - \frac{1}{\mid G \mid^{1/3}}\left(G - \frac{J_1}{3}I\right)\right)\end{aligned} \tag{33}$$

Here

$$p = \rho^2 \frac{\partial \varepsilon}{\partial \rho}$$

is the thermodynamic pressure. Obviously,

$$p = -\frac{tr(\sigma)}{3}$$

Hence, the shear part of the energy has no influence on the pressure, it is determined only by the hydrodynamic part. For this form of the energy, the shear part of the stress tensor has always zero trace. In the case of small displacements, we obtain the classical Hooke law.

3.3. Governing equations

The governing equations can be written in the form:

$$\frac{\partial \mathbf{e}^\alpha}{\partial t} + \nabla(\mathbf{v}\cdot\mathbf{e}^\alpha) = 0, \quad \mathrm{rot}\,\mathbf{e}^\alpha = 0,$$
$$\frac{\partial \rho}{\partial t} + \mathrm{div}(\rho\mathbf{v}) = 0,$$
$$\frac{\partial \rho\mathbf{v}}{\partial t} + \mathrm{div}(\rho\mathbf{v}\otimes\mathbf{v} - \sigma) = \rho\mathbf{f},$$
$$\frac{\partial (\rho E)}{\partial t} + \mathrm{div}(\rho\mathbf{v}E - \sigma\mathbf{v}) = \rho\mathbf{v}\cdot\mathbf{f}.$$

Here $E = \varepsilon + \varepsilon_e + \frac{\mathbf{v}\cdot\mathbf{v}}{2}$ is the specific total energy, $\mathbf{f}$ is the specific external force. Initial conditions for $\mathbf{e}^\alpha$ are:

$$\mathbf{e}^\alpha|_{t=0} = \mathbf{i}^\alpha, \quad \alpha = 1,2,3$$

where $\mathbf{i}^\alpha$ are the vectors of Cartesian basis.

3.4. Hyperbolicity

For the sake of simplicity, we will suppose that the specific entropy s and the Lagrangian density ρ_0 which conserve along trajectories

$$\frac{Ds}{Dt} = 0, \quad \frac{D\rho_0}{Dt} = 0,$$

are constant. Indeed, these equations give only contact characteristics. Since the density can be expressed in terms of G by

$$\rho = \rho_0 \mid G\mid^{1/2}$$

we will not consider the density as independent variable. To avoid the double indices, we introduce the following notation:

$$\mathbf{e}^\alpha = \begin{pmatrix} e_1^\alpha \\ e_2^\alpha \\ e_3^\alpha \end{pmatrix} = \begin{pmatrix} a^\alpha \\ b^\alpha \\ c^\alpha \end{pmatrix}, \quad \alpha = 1,2,3$$

The matrix G is then

$$G = \begin{pmatrix} (a^1)^2 + (a^2)^2 + (a^3)^2 & a^1b^1 + a^2b^2 + a^3b^3 & a^1c^1 + a^2c^2 + a^3c^3 \\ a^1b^1 + a^2b^2 + a^3b^3 & (b^1)^2 + (b^2)^2 + (b^3)^2 & b^1c^1 + b^2c^2 + b^3c^3 \\ a^1c^1 + a^2c^2 + a^3c^3 & b^1c^1 + b^2c^2 + b^3c^3 & (c^1)^2 + (c^2)^2 + (c^3)^2 \end{pmatrix}$$

The equations

$$\frac{\partial \mathbf{e}^\alpha}{\partial t} + \nabla(\mathbf{v}\cdot\mathbf{e}^\alpha) = 0, \quad \operatorname{rot}\mathbf{e}^\alpha = 0$$

in Cartesian coordinates are

$$\frac{\partial a^\alpha}{\partial t} + \frac{\partial}{\partial x}(ua^\alpha + vb^\alpha + wc^\alpha) = 0, \quad \frac{\partial b^\alpha}{\partial t} + \frac{\partial}{\partial y}(ua^\alpha + vb^\alpha + wc^\alpha) = 0, \quad \frac{\partial c^\alpha}{\partial t} + \frac{\partial}{\partial z}(ua^\alpha + vb^\alpha + wc^\alpha) = 0,$$
$$\frac{\partial b^\alpha}{\partial x} - \frac{\partial a^\alpha}{\partial y} = 0, \quad \frac{\partial a^\alpha}{\partial z} - \frac{\partial c^\alpha}{\partial x} = 0, \quad \frac{\partial c^\alpha}{\partial y} - \frac{\partial b^\alpha}{\partial z} = 0.$$

Here $\mathbf{v} = (u, v, w)^{\mathrm{T}}$. If all the variables depend only on (t, x) this imply that

$$b^\alpha = \text{const}, \quad c^\alpha = \text{const},$$

and, since initially $b^1 = 0$, $c^1 = 0$, $b^2 = 1$, $c^2 = 0$, $b^3 = 0$, $c^3 = 1$, we obtain

$$G = \begin{pmatrix} (a^1)^2 + (a^2)^2 + (a^3)^2 & a^2 & a^3 \\ a^2 & 1 & 0 \\ a^3 & 0 & 1 \end{pmatrix}, \quad |G| = (a^1)^2, \quad J_1 = (a^1)^2 + (a^2)^2 + (a^3)^2 + 2$$

Hence

$$\rho = \rho_0 |G|^{1/2} = a^1\rho_0$$

The stress tensor is

$$\sigma = \begin{pmatrix} \sigma_{11} & \sigma_{12} & \sigma_{13} \\ \sigma_{12} & \sigma_{22} & \sigma_{23} \\ \sigma_{13} & \sigma_{23} & \sigma_{33} \end{pmatrix}.$$

The governing equations are

$$\begin{aligned} &\frac{\partial a^1}{\partial t} + \frac{\partial}{\partial x}(ua^1) = 0, \\ &\frac{\partial a^2}{\partial t} + \frac{\partial}{\partial x}(ua^2 + v) = 0, \\ &\frac{\partial a^3}{\partial t} + \frac{\partial}{\partial x}(ua^3 + w) = 0, \\ &\frac{\partial u}{\partial t} + u\frac{\partial u}{\partial x} - \frac{1}{\rho}\frac{\partial \sigma_{11}}{\partial x} = 0, \\ &\frac{\partial v}{\partial t} + u\frac{\partial v}{\partial x} - \frac{1}{\rho}\frac{\partial \sigma_{12}}{\partial x} = 0, \\ &\frac{\partial w}{\partial t} + u\frac{\partial w}{\partial x} - \frac{1}{\rho}\frac{\partial \sigma_{13}}{\partial x} = 0. \end{aligned} \tag{34}$$

The conservative form of (34) is

$$\begin{aligned} &\frac{\partial a^1}{\partial t} + \frac{\partial}{\partial x}(ua^1) = 0, \\ &\frac{\partial a^2}{\partial t} + \frac{\partial}{\partial x}(ua^2 + v) = 0, \\ &\frac{\partial a^3}{\partial t} + \frac{\partial}{\partial x}(ua^3 + w) = 0, \\ &\frac{\partial (a^1\rho_0 u)}{\partial t} + \frac{\partial}{\partial x}(a^1\rho_0(u)^2 - \sigma_{11}) = 0, \end{aligned}$$

$$\frac{\partial(a^1\rho_0 v)}{\partial t}+\frac{\partial}{\partial x}(a^1\rho_0 uv-\sigma_{12})=0,$$
$$\frac{\partial(a^1\rho_0 w)}{\partial t}+\frac{\partial}{\partial x}(a^1\rho_0 uw-\sigma_{13})=0, \tag{35}$$

Introducing the vector of unknowns

$$\mathbf{V}=\begin{pmatrix} a^1\\ a^2\\ a^3\\ u\\ v\\ w\end{pmatrix}$$

we rewrite system (34) in the form

$$\frac{\partial \mathbf{V}}{\partial t}+A(\mathbf{V})\frac{\partial \mathbf{V}}{\partial x}=0$$

where the matrix $A(\mathbf{V})$ is given by

$$A(\mathbf{V})=\begin{pmatrix} u & 0 & 0 & a^1 & 0 & 0\\ 0 & u & 0 & a^2 & 1 & 0\\ 0 & 0 & u & a^3 & 0 & 1\\ -\frac{1}{\rho}\frac{\partial\sigma_{11}}{\partial a^1} & -\frac{1}{\rho}\frac{\partial\sigma_{11}}{\partial a^2} & -\frac{1}{\rho}\frac{\partial\sigma_{11}}{\partial a^3} & u & 0 & 0\\ -\frac{1}{\rho}\frac{\partial\sigma_{12}}{\partial a^1} & -\frac{1}{\rho}\frac{\partial\sigma_{12}}{\partial a^2} & -\frac{1}{\rho}\frac{\partial\sigma_{12}}{\partial a^3} & 0 & u & 0\\ -\frac{1}{\rho}\frac{\partial\sigma_{13}}{\partial a^1} & -\frac{1}{\rho}\frac{\partial\sigma_{13}}{\partial a^2} & -\frac{1}{\rho}\frac{\partial\sigma_{13}}{\partial a^3} & 0 & 0 & u\end{pmatrix}$$

In the limit of small displacements we obtain the following eigenvalues

$$v_{1,2,3,4}=u\pm\sqrt{\frac{\mu}{\rho_0}},\quad v_{5,6}=u\pm\sqrt{c_0^2+\frac{4\mu}{3\rho_0}}$$

In particular, if we take c_0^2 as

$$c_0^2=\frac{3\lambda+2\mu}{3\rho_0}$$

where λ and μ are the Lamé coefficients, we obtain classical velocities of transverse and longitudinal waves:

$$v_{1,2,3,4}=u\pm\sqrt{\frac{\mu}{\rho_0}},\quad v_{5,6}=u\pm\sqrt{\frac{\lambda+2\mu}{\rho_0}}$$

Hence, the system is hyperbolic in the vicinity of the equilibrium state

$$a^1=1,\quad a^2=0,\quad a^3=0$$

To find eigenvalues explicitly, we consider the case where $a^3=0$, and $w=0$. The matrix G will be:

$$G=\begin{pmatrix}(a^1)^2+(a^2)^2 & a^2 & 1\\ a^2 & 1 & 0\\ 1 & 0 & 1\end{pmatrix}$$

The matrix $A(\mathbf{V})$ will be then 4×4 matrix:

$$A(\mathbf{V}) = \begin{pmatrix} u & 0 & a^1 & 0 \\ 0 & u & a^2 & 1 \\ -\frac{1}{\rho}\frac{\partial \sigma_{11}}{\partial a^1} & -\frac{1}{\rho}\frac{\partial \sigma_{11}}{\partial a^2} & u & 0 \\ -\frac{1}{\rho}\frac{\partial \sigma_{12}}{\partial a^1} & -\frac{1}{\rho}\frac{\partial \sigma_{12}}{\partial a^2} & 0 & u \end{pmatrix}$$

The eigenvalues of the matrix $A(\mathbf{V})$ are given by

$$\det(A - vI) = 0$$

They are the solutions of the following polynomial of the fourth degree and can be found in explicit form:

$$(u-v)^4 + \left(\frac{a^1\sigma_{11,1} + \sigma_{12,2}(1+a^2)}{\rho}\right)(u-v)^2 + a^1\left(\frac{\sigma_{11,1}\sigma_{12,2} - \sigma_{12,1}\sigma_{11,2}}{\rho^2}\right) = 0 \tag{36}$$

Here

$$\sigma_{ij,\alpha} = \frac{\partial \sigma_{ij}}{\partial a^\alpha}$$

Explicit formulae for the coefficients of this polynomial can be found in Appendix 1.

3.5. Fully conservative elasticity model in 1D case

Using the equation for the reference density ρ_0

$$\frac{D\rho_0}{Dt} = 0$$

the governing equations can be rewritten in the following conservative form

$$\begin{aligned}
&\frac{\partial(\rho_0 a^1)}{\partial t} + \frac{\partial}{\partial x}\left(\rho_0 a^1 u\right) = 0,\\
&\frac{\partial a^2}{\partial t} + \frac{\partial}{\partial x}(u a^2 + v) = 0,\\
&\frac{\partial a^3}{\partial t} + \frac{\partial}{\partial x}(u a^3 + w) = 0,\\
&\frac{\partial(a^1\rho_0 u)}{\partial t} + \frac{\partial}{\partial x}\left(a^1\rho_0 (u)^2 - \sigma_{11}\right) = 0,\\
&\frac{\partial(a^1\rho_0 v)}{\partial t} + \frac{\partial}{\partial x}\left(a^1\rho_0 uv - \sigma_{12}\right) = 0,\\
&\frac{\partial(a^1\rho_0 w)}{\partial t} + \frac{\partial}{\partial x}\left(a^1\rho_0 uw - \sigma_{13}\right) = 0,\\
&\frac{\partial(a^1\rho_0 E)}{\partial t} + \frac{\partial}{\partial x}\left(a^1\rho_0 uE - \sigma_{11}u - \sigma_{12}v - \sigma_{13}w\right) = 0.
\end{aligned} \tag{37}$$

Here

$$E = e + \frac{1}{2}(u^2 + v^2 + w^2) = \varepsilon(\rho, s) + \varepsilon_e(g, s) + \frac{1}{2}(u^2 + v^2 + w^2),$$

where $\varepsilon(\rho, s)$ and $\varepsilon_e(g, s)$ are given by (31) and (32). The expressions for components of the stress tensor follow from (33) (see also Appendix 1).

We note that the system can be symmetrized, if ρe is a convex function of $(\rho, a^2, a^3, \rho s)$ [3,5,6].

Typical solutions of system (37) will be examined and compared with the "exact" solution of the non-conservative model (5). To this end, a numerical method will be used to solve system (37).

4. Numerical method

The aim of this section is to derive a second-order Godunov scheme with approximate Riemann solver. The HLLC approximate solver [17] is used to compute the fluxes at cell boundaries.

4.1. HLLC solver

This solver considers each wave as a discontinuity. In the HLLC framework, only two extreme waves and the contact discontinuity are considered. It means that only two intermediate states instead of four will be considered. Examination of the results will show that such approximation has no serious consequences.

Each wave being considered as a discontinuity and the system being conservative, Rankine–Hugoniot conditions across each wave (S_L, S_R and S^*) read:

$$\mathbf{F}_L^* - S_L^* \mathbf{U}_L^* = \mathbf{F}_L - S\mathbf{U}_L = \mathbf{Q}_L, \tag{38}$$

$$\mathbf{F}_R^* - S_R \mathbf{U}_R^* = \mathbf{F}_R - S_R \mathbf{U}_R = \mathbf{Q}_R, \tag{39}$$

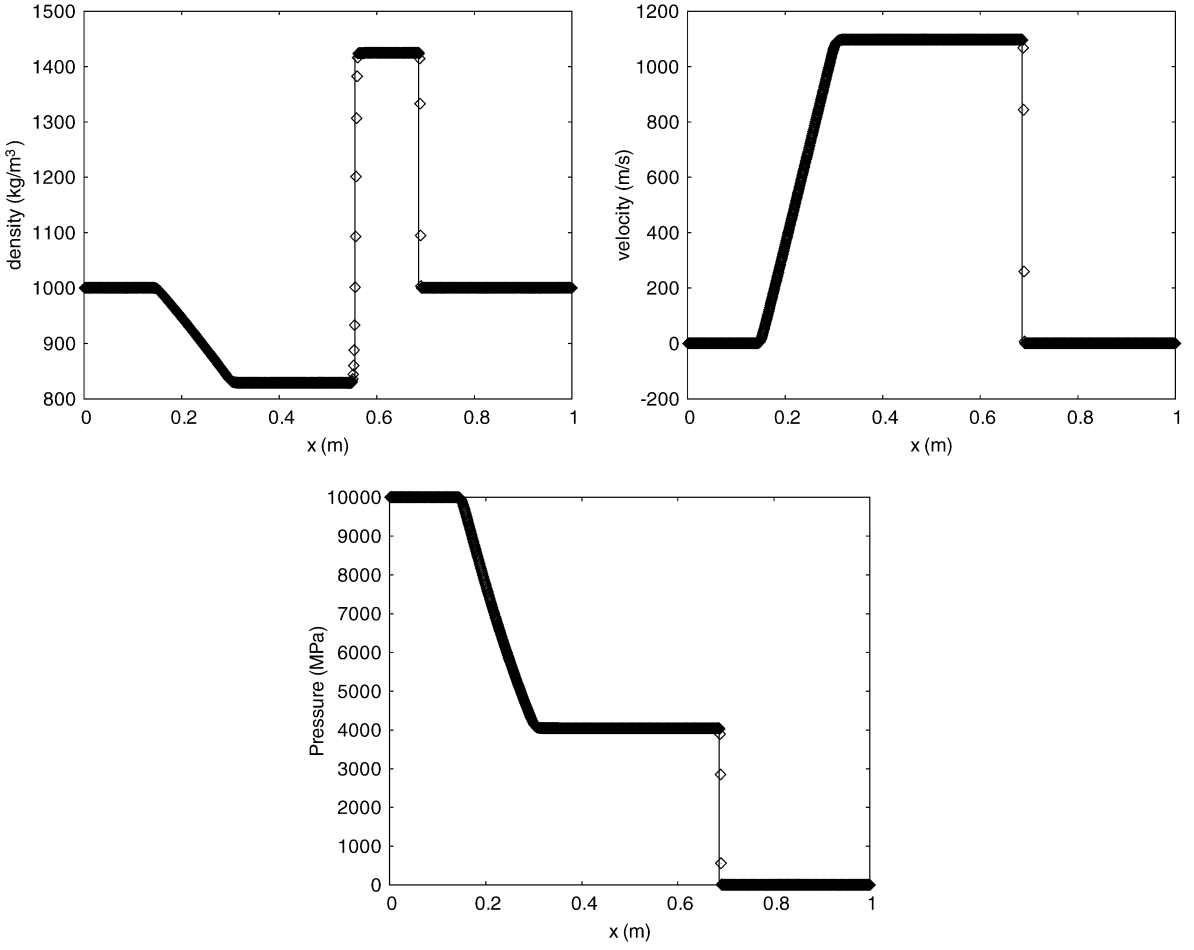

Fig. 5. Shock tube test problem in the fluid limit. The numerical solution of the conservative model is shown with symbols. It is compared to the exact solution shown with lines at time $t = 51$ μs. The agreement is perfect.

$$\mathbf{F}_{\mathrm{R}}^{*}-S^{*}\mathbf{U}_{\mathrm{R}}^{*}=\mathbf{F}_{\mathrm{L}}^{*}-S^{*}\mathbf{U}_{\mathrm{L}}^{*},$$

$$\text{where } \mathbf{U}=\begin{pmatrix} a^{1} \\ a^{1}\rho_{0} \\ a^{2} \\ a^{1}\rho_{0}u \\ a^{1}\rho_{0}v \\ a^{1}\rho_{0}E \\ a^{3} \\ a^{1}\rho_{0}w \end{pmatrix} \quad \text{and} \quad \mathbf{F}=\begin{pmatrix} a^{1}u \\ a^{1}\rho_{0}u \\ a^{2}u+v \\ a^{1}\rho_{0}u^{2}-\sigma_{11} \\ a^{1}\rho_{0}vu-\sigma_{12} \\ a^{1}\rho_{0}Eu-\sigma_{11}u-\sigma_{12}v-\sigma_{13}w \\ a^{3}u+w \\ a^{1}\rho_{0}wu-\sigma_{13} \end{pmatrix}.$$

The extreme wave speeds are approximated by [2]:

$$\begin{aligned} S_{\mathrm{L}} &= \min(u_{\mathrm{R}}-c_{\mathrm{R}},u_{\mathrm{L}}-c_{\mathrm{L}}), \\ S_{\mathrm{R}} &= \max(u_{\mathrm{R}}+c_{\mathrm{R}},u_{\mathrm{L}}+c_{\mathrm{L}}), \end{aligned} \tag{40}$$

where c_{R} and c_{L} are the sound speeds corresponding to largest roots of the polynomial (36). The intermediate wave speed is obtained under HLL approximation [8]:

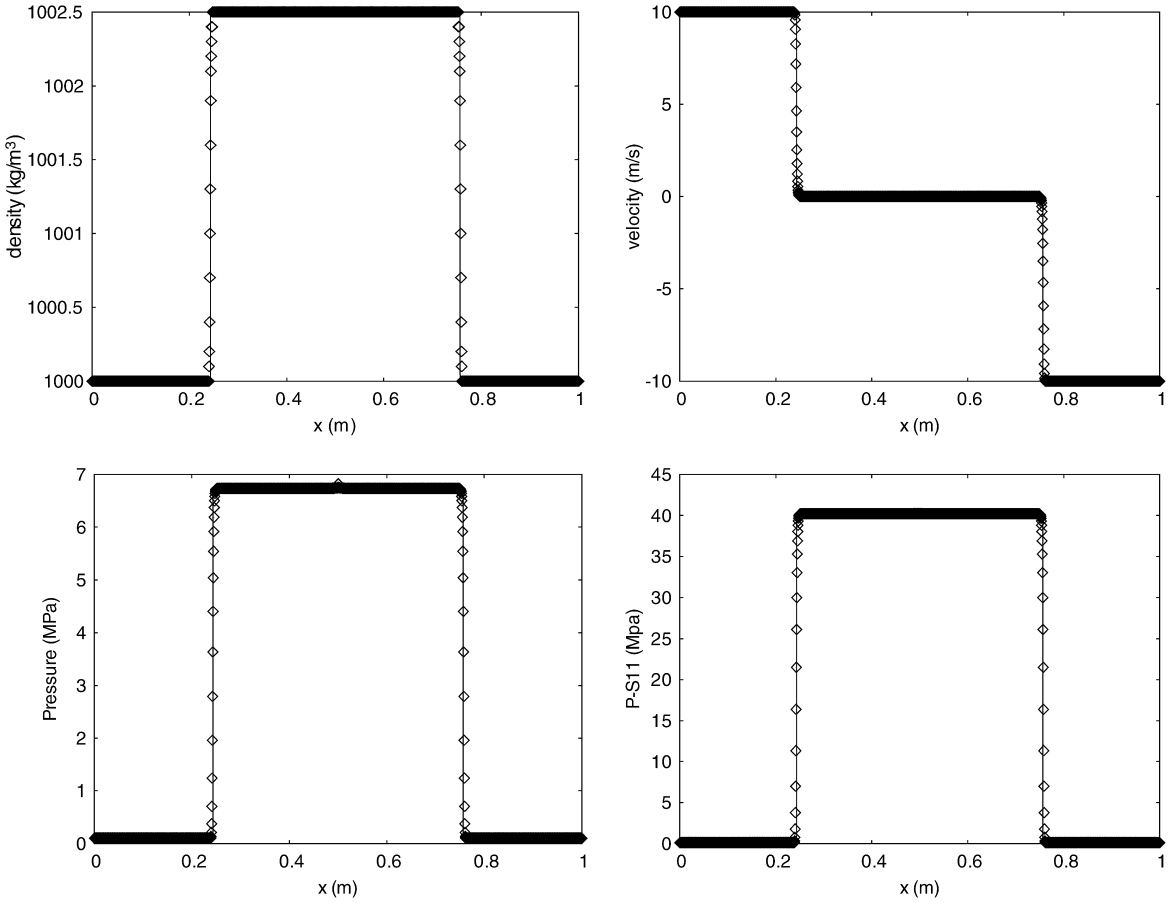

Fig. 6. Impact test problem with elastic materials with the initial velocity difference of 20 m/s.The exact solution with the non-conservative model is shown with lines and the numerical solution with the conservative model is shown with symbols. A 2000 cells mesh is used. Both solutions are in perfect agreement.

$$S^* = u^* = u_L^* = u_R^* = \frac{Q_R(4) - Q_L(4)}{Q_R(2) - Q_L(2)} \tag{41}$$

In the following, $Q_R(i)$ (or $Q_L(i)$) denotes the ith component of the vector $\mathbf{Q}_R$ (or $\mathbf{Q}_L$). Using relations (38), (39) the intermediate states are obtained as:

$$a_L^{1*} = \frac{Q_L(1)}{S^* - S_L}, \quad a_R^{1*} = \frac{Q_R(1)}{S^* - S_R},$$
$$\sigma_{11}^* = \sigma_{11L}^* = \sigma_{11R}^* = \frac{Q_L(2)Q_R(4) - Q_R(2)Q_L(4)}{Q_R(2) - Q_L(2)},$$
$$\sigma_{12}^* = \sigma_{12L}^* = \sigma_{12R}^* = \frac{Q_R(2)Q_L(5) - Q_L(2)Q_R(5)}{Q_L(2) - Q_R(2)},$$
$$v^* = v_L^* = v_R^* = \frac{Q_L(5) - Q_R(5)}{Q_L(2) - Q_R(2)},$$
$$a_L^{2*} = \frac{Q_L(3) - v^*}{S^* - S_L}, \quad a_R^{2*} = \frac{Q_R(3) - v^*}{S^* - S_R},$$
$$E_L^* = \frac{Q_L(6) + \sigma_{11}^* u^* + \sigma_{12}^* v^*}{Q_L(2)}, \quad E_R^* = \frac{Q_R(6) + \sigma_{11}^* u^* + \sigma_{12}^* v^*}{Q_R(2)}$$

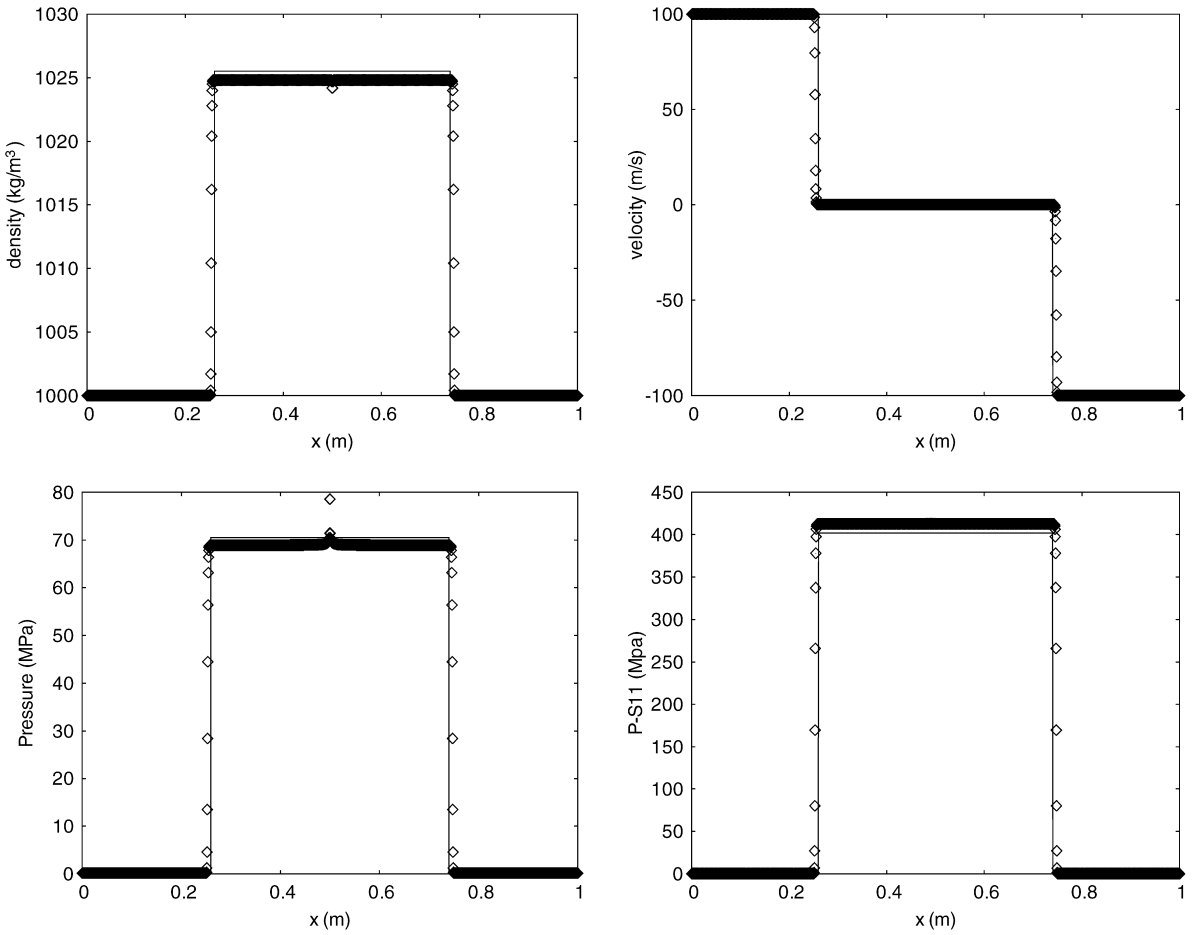

Fig. 7. Impact test problem with elastic materials with the initial velocity differential of 200 m/s. The exact solution with the non-conservative model is shown with lines and the numerical solution with the conservative model is shown with symbols. A 2000 cells mesh is used. Slight differences appear.

The flux for the Godunov method is sampled as follows:

$$\mathbf{F}_{i+1/2}^{\mathrm{HLLC}} = \begin{cases} \mathbf{F}_{\mathrm{L}} \text{ if } 0 \leqslant S_{\mathrm{L}} \\ \mathbf{F}_{\mathrm{L}}^{*} = \mathbf{F}_{\mathrm{L}} + S_{\mathrm{L}}\left(\mathbf{U}_{\mathrm{L}}^{*} - \mathbf{U}_{\mathrm{L}}\right) \text{ if } S_{\mathrm{L}} \leqslant 0 \leqslant S^{*} \\ \mathbf{F}_{\mathrm{R}}^{*} = \mathbf{F}_{\mathrm{L}} + S_{\mathrm{R}}\left(\mathbf{U}_{\mathrm{R}}^{*} - \mathbf{U}_{\mathrm{R}}\right) \text{ if } S^{*} \leqslant 0 \leqslant S_{\mathrm{R}} \\ \mathbf{F}_{\mathrm{R}} \text{ if } 0 \geqslant S_{\mathrm{R}} \end{cases}.$$

4.2. Second-order Godunov type scheme

The second-order Godunov type method used for the computation of the forthcoming section follows MUSCL-Hancock method (see [18]. The flow variables are characterized by a mean value $\mathbf{U}_i^n$ and a slope $\delta\mathbf{U}_i^n$. The slopes are here computed with conservative variables $\mathbf{U}$, but other options are possible. The conservative variables at the cell boundary are given by: $\mathbf{U}_{i+1/2,-}^n = \mathbf{U}_i^n + \frac{1}{2}\delta\mathbf{U}_i^n$ and $\mathbf{U}_{i-1/2,+}^n = \mathbf{U}_i^n - \frac{1}{2}\delta\mathbf{U}_i^n$

These cell boundary variables are then evolved over half a time step by:

$$\mathbf{U}_{i+1/2,-}^{n+1/2} = \mathbf{U}_{i+1/2,-}^n - \frac{\Delta t}{2\Delta x}\left(\mathbf{F}_{i+1/2}^n - \mathbf{F}_{i-1/2}^n\right),$$

$$\mathbf{U}_{i-1/2,+}^{n+1/2} = \mathbf{U}_{i-1/2,+}^n - \frac{\Delta t}{2\Delta x}\left(\mathbf{F}_{i+1/2}^n - \mathbf{F}_{i-1/2}^n\right).$$

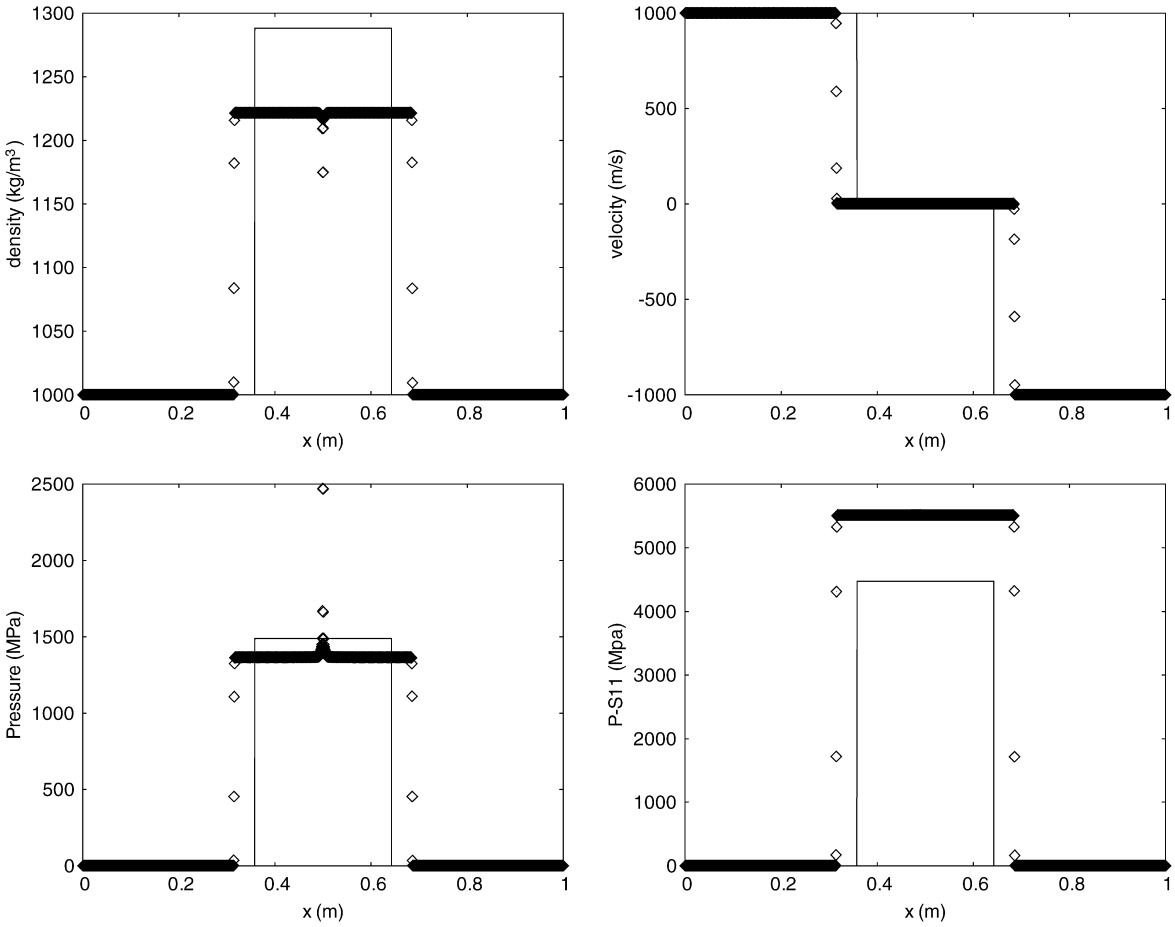

Fig. 8. Impact test problem with elastic materials with the initial velocity difference of 2000 m/s. The exact solution with the non-conservative model is shown with lines and the numerical solution with the conservative model is shown with symbols. A 2000 cells mesh is used. Large differences appear.

The Riemann problem under HLLC approximation is then solved with cell boundary states $\mathbf{U}^{n+1/2}_{i\pm1/2,-}$ and $\mathbf{U}^{n+1/2}_{i\pm1/2,+}$ as initial data. The solution is then evolved over the time step:

$$\mathbf{U}_i^{n+1} = \mathbf{U}_i^n - \frac{\Delta t}{\Delta x}\left(\mathbf{F}^{\mathrm{HLLC}}\left(\mathbf{U}^{n+1/2}_{i+1/2,-}, \mathbf{U}^{n+1/2}_{i+1/2,+}\right) - \mathbf{F}^{\mathrm{HLLC}}\left(\mathbf{U}^{n+1/2}_{i-1/2,-}, \mathbf{U}^{n+1/2}_{i-1/2,+}\right)\right)$$

Results presented in the following section are obtained by using [20, limiter].

5. Numerical results

In this section, the exact solution of the non-conservative model presented in Section 2 is compared to the numerical solution of the conservative model developed in Section 3. In the conservative model shear effects are coupled with longitudinal waves, while they are uncoupled in the non-conservative model. Hence, a formal comparison with mathematical formulations of the two models cannot be done. It is the reason why a comparison of their numerical solutions is important.

The numerical results presented for the conservative model of Section 3 are obtained with the numerical scheme presented in Section 4. The material is governed by the stiffened gas EOS with parameters $p_\infty = 6\ 10^8$ Pa, $\gamma = 4.4$.

5.1. Fluid limit

In this example the shear modulus μ in both models is set to zero. Both flow models reduce to the Euler equations. We consider a shock tube where an interface separates initially a material at rest with high pressure $p = 10^{10}$ Pa and density $\rho = 1000$ kg/m^3 on the left, and the same material at rest with low pressure $p = 10^5$ Pa and density $\rho = 1000$ kg/m^3 on the right. The interface is initially located at $x_i = 0.5$ m. Fig. 5 shows computed results at time $t = 51$ μs. Symbols correspond to the numerical solution of the conservative model, the exact solution is shown with lines. A perfect agreement is observed in Fig. 5.

5.2. Shocks in elastic materials

In the following test problems the material is considered elastic with a shear modulus $\mu = 10^{10}$ Pa.

The Riemann problem with two colliding materials is considered under three different impact velocity difference: 20 m/s, 200 m/s and 2000 m/s. The materials have in all tests the same initial pressure ($p = 10^5$ Pa),

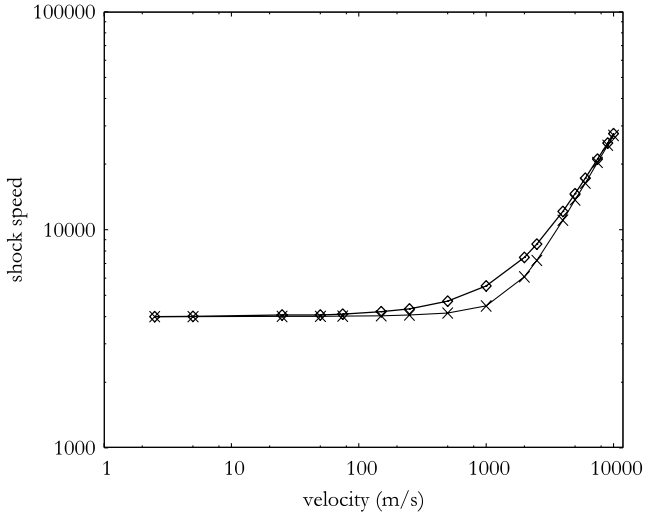

Fig. 9. Shock velocity – particle velocity relation is shown for the two models (conservative with square symbols, non-conservative with cross symbols). Both models have the same weak and strong shocks limits. But differences are present for shocks of intermediate strength.

the same initial density ($\rho = 1000\ \mathrm{kg/m^3}$) and zero initial shear stress ($S = 0$). Impacts of the two materials occurs at $x_i = 0.5$ m.

Fig. 6 shows a comparison between "exact" results from the non-conservative model (lines) and numerical results of the conservative model (symbols) in the weak shock limit (the initial velocity difference is 20 m/s).

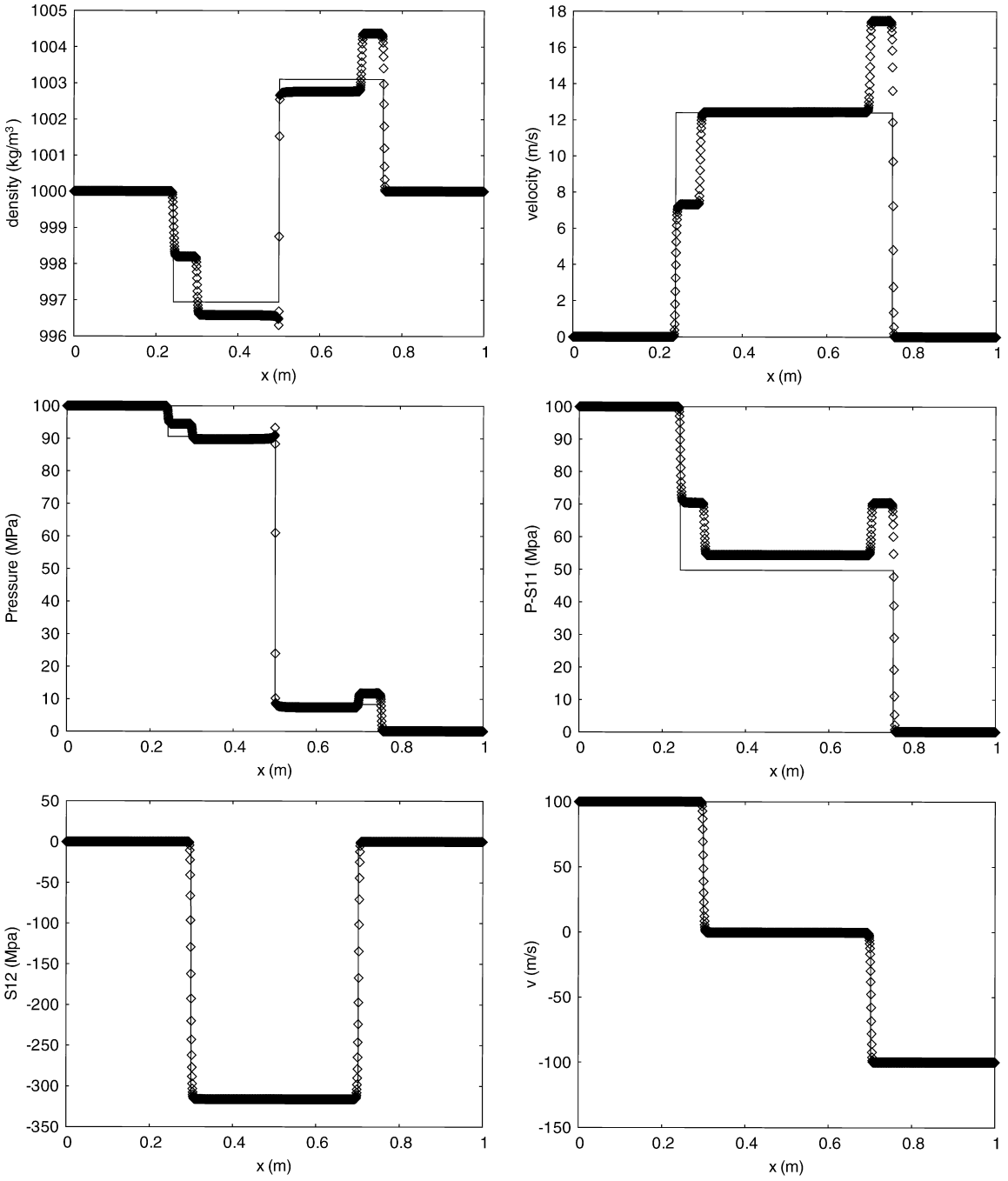

Fig. 10. The material is considered elastic with $\mu = 10^{10}$ Pa in the presence of an initial tangential velocity discontinuity. The numerical solution of the conservative model is shown with symbols and the exact solution of the non-conservative model is shown with lines at time $t = 64$ μs. Five waves are visible: the three classical waves (rarefaction on the left, shock wave on the right and the contact discontinuity) and two shear waves. Large differences between the two models are clearly visible.

The output time is $t = 64$ μs. As the results are in perfect agreement, we can conclude that both models have the same weak shock limit.

We now consider stronger shocks. Fig. 7 shows a comparison between "exact" results from the non-conservative model and numerical results of the conservative one (symbols) for shocks of moderate strength (the initial velocity difference is 200 m/s). The output time is $t = 61$ μs. Slight differences appear in the wave speeds and post-shock states.

We now consider strong shocks. Fig. 8 shows a comparison between "exact" results from the non-conservative model and numerical results of the conservative one (symbols) for strong shocks (the initial velocity difference is 2000 m/s). The output time is $t = 41$ μs. Large differences appear in the wave speeds and post-shock states.

It is interesting to note that these differences vanish when the shocks become much stronger. In Fig. 9 the shock velocity (in log scale) as a function of the material velocity (in log scale) is shown for both models. It appears clearly that both models have the same weak and strong shocks limits. But for intermediate shocks, differences are present.

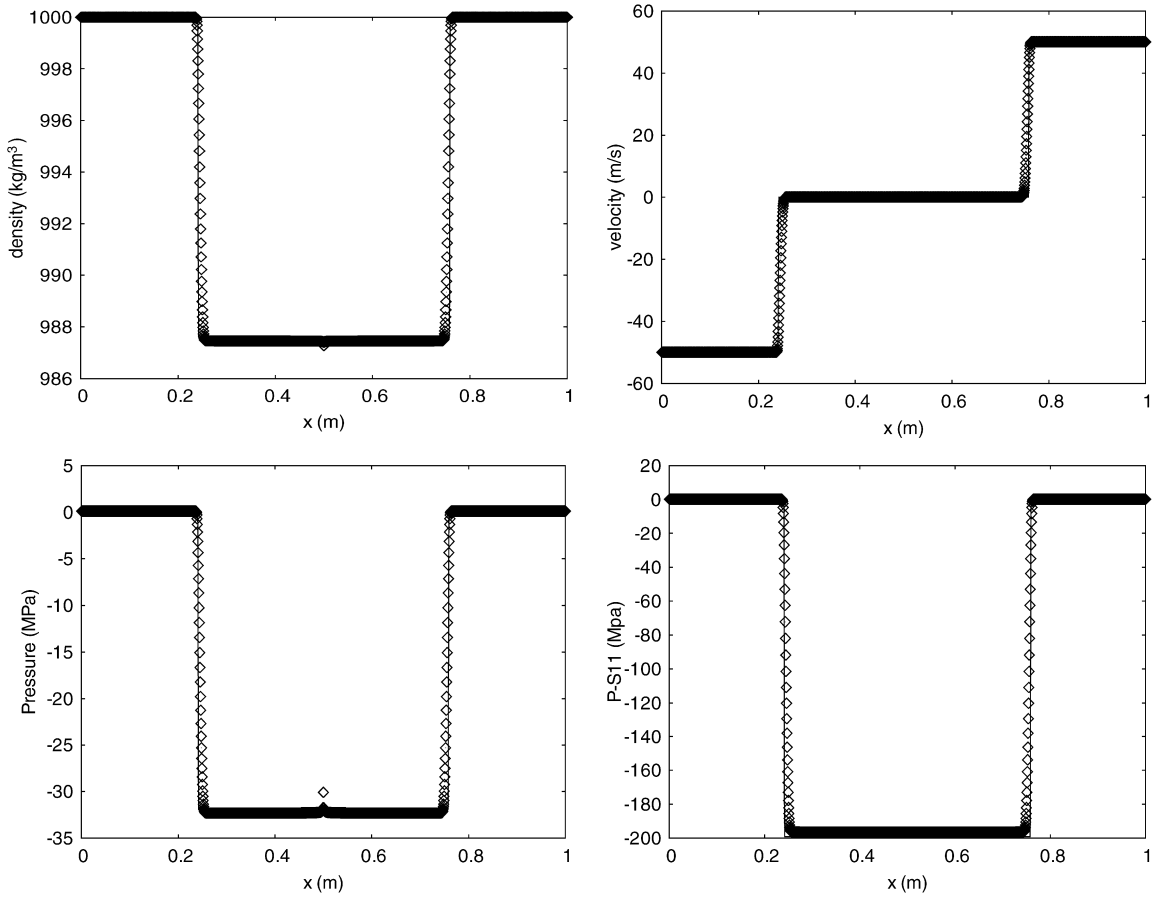

Fig. 11. Expansion wave problem. The material is considered elastic with $\mu = 10^{10}$ Pa. The initial velocity is $u = -50$ m/s on the left ($x < 0.5$ m). On the right ($x > 0.5$ m), the initial velocity is set to $u = 50$ m/s. Computed results with the conservative model are shown with symbols at time $t = 64$ μs. The exact solution of the non-conservative model is shown with lines. For weak expansion waves, the agreement with both models is perfect.

5.3. Configurations with five waves

In presence of shear effects, five waves are expected. The material is considered elastic with a shear modulus $\mu = 10^{10}$ Pa. An interface separates initially the material with high pressure $p = 10^8$ Pa and density $\rho = 1000\ \mathrm{kg/m^3}$ on the left, and the same material at rest with pressure $p = 10^5$ Pa and density $\rho = 1000\ \mathrm{kg/m^3}$ on the right. A tangential velocity discontinuity is imposed: $v = 100$ m/s on the left and $v = -100$ m/s on the right. The interface is initially located at $x_i = 0.5$ m. Fig. 10 shows computed results at time $t = 64$ μs. A large difference between models is clearly visible. Let us remark that wave patterns with five waves have been also reported by [16] using the Godunov model close to the conservative model proposed in Section 3.

5.4. Expansion waves

Preceding examples clearly show the differences between the two models in presence of shocks and shear waves. We now examine their behavior for weak and strong expansion waves. The same elastic material as previously is considered. The initial pressure is $p = 10^5$ Pa and the initial density is $\rho = 1000\ \mathrm{kg/m^3}$ everywhere.

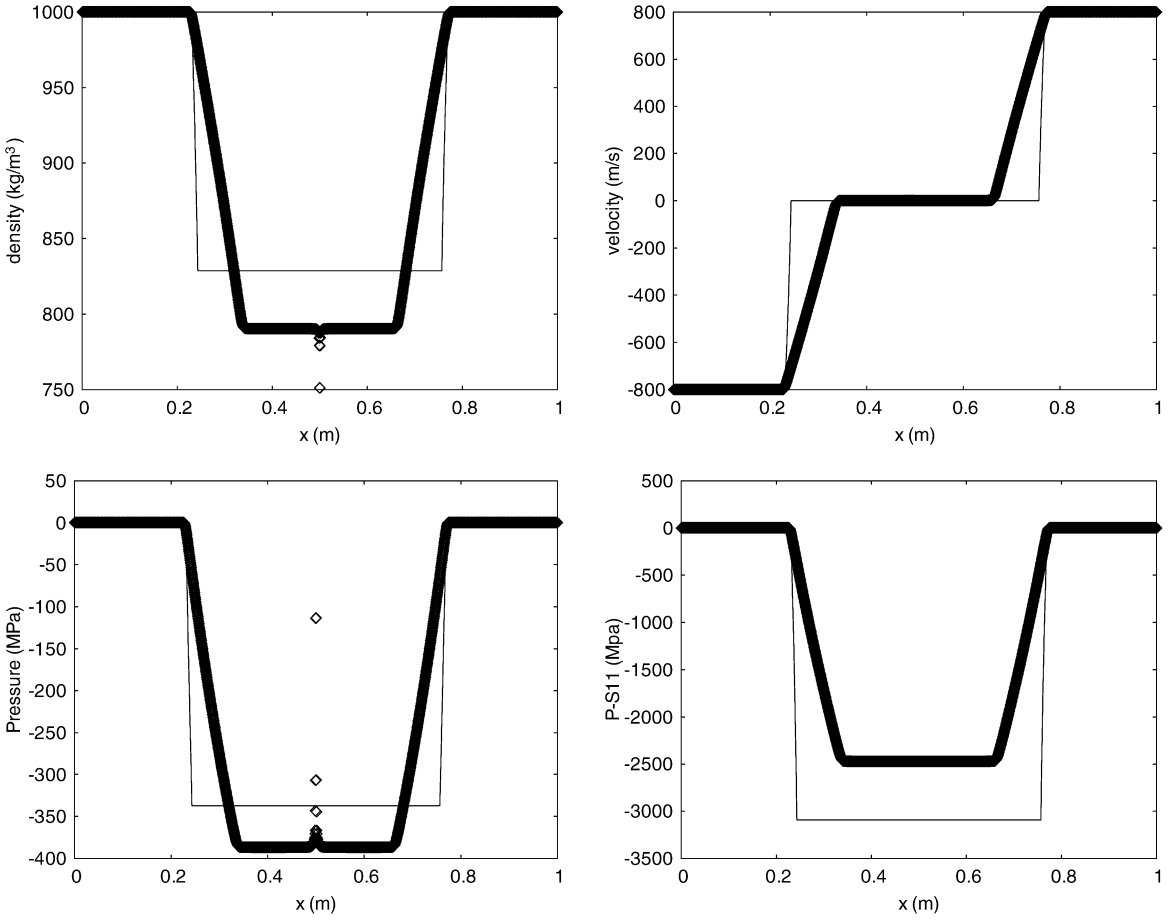

Fig. 12. Expansion wave problem. The material is considered elastic with $\mu = 10^{10}$ Pa. The initial velocity is $u = -800$ m/s on ($x < 0.5$ m). On the right ($x > 0.5$ m), the initial velocity is set to $u = 800$ m/s. Computed results with the conservative model are shown with symbols at time $t = 40$ μs. Exact solution of the non-conservative model is shown with lines. For strong expansion waves large differences are present.

In the first run, the initial velocity is $u = -50$ m/s on the left part of the domain ($x < 0.5$ m). On the right, the initial velocity is set to $u = 50$ m/s. Computed results with the conservative model are shown with symbols in the Fig. 11 at time $t = 64$ μs. The exact solution of the non-conservative model is shown with lines. For weak expansion waves, the agreement is perfect.

We now consider stronger expansion waves. The same initial data are used except the velocity in the left chamber, now set to $u = -800$ m/s and the velocity in the right chamber set to $u = 800$ m/s. Computed results with the conservative model are shown with symbols in the Fig. 12 at time $t = 40$ μs. Exact solution of the non-conservative model is shown with lines. For strong expansion waves large differences are present.

It is important to recall that both models are isentropic in absence of shocks. However, the non-conservative model is based on assumption of small deformations. Consequently, under strong variations (shocks and expansions) the non-conservative flow model predictions are questionable.

6. Conclusion

A modified version of [5,10] model for compressible elastic materials subjected to large deformations has been studied. It represents a conservative hyperbolic system able to deal with strong shocks and large amplitude expansion waves. Typical solutions of this model are compared with solutions of a more conventional Eulerian non-conservative model. The numerical results for different tests show good agreement of both models for waves of very small or very large amplitude. However, for waves of intermediate amplitude there are important discrepancies between results.

The topic of interfaces separating elastic bodies and compressible fluids encountered in multiple applications has not been addressed here. The paper by [11] gives a relevant example where such a problem has been studied. The relaxation-projection method developed in [12,15] can be examined for the computation of such interface problems.

Acknowledgments

S.G. and R.S. have been largely benefited from the discussion with Professor S.K. Godunov during his visit to l'IUSTI, Marseille. The authors thank anonymous referees for important remarks and suggestions.

Appendix 1. Wave speed calculation

The internal energy is taken in the form

$$e = \varepsilon(\rho, s) + \varepsilon_e(J_1, J_2, s)$$

where

$$\varepsilon(\rho,p) = \frac{p + \gamma p_\infty}{\rho(\gamma - 1)}, \quad p + p_\infty = \exp\left(\frac{s - s_0}{c_v}\right)\rho^\gamma, \quad s_0 = \text{const}, \quad \varepsilon_e(g,s) = \frac{\mu}{4\rho_0} tr((g - I)^2)$$

$$= \frac{\mu}{4\rho_0} tr\left(\frac{1}{(a^1)^{4/3}}\begin{pmatrix} (a^1)^2 - (a^1)^{2/3} + (a^2)^2 + (a^3)^2 & a^2 & a^3 \\ a^2 & 1 - (a^1)^{2/3} & 0 \\ a^3 & 0 & 1 - (a^1)^{2/3} \end{pmatrix}^2\right), \quad g = \frac{G}{|G|^{1/3}}$$

and

$$G = \begin{pmatrix} (a^1)^2 + (a^2)^2 + (a^3)^2 & a^2 & a^3 \\ a^2 & 1 & 0 \\ a^3 & 0 & 1 \end{pmatrix}$$

Calculations give us explicit expression of ε_e:

$$\varepsilon_e = \frac{\mu}{4\rho_0}\frac{1}{(a^1)^{4/3}}(((a^1)^2 - (a^1)^{2/3} + (a^2)^2 + (a^3)^2)^2 + 2(1 - (a^1)^{2/3})^2 + 2((a^2)^2 + (a^3)^2))$$

The stress tensor is given by

$$\sigma = -pI - \mu\left(\frac{G^2 - \frac{J_2}{3}I}{(a^1)^{1/3}} - \left(G - \frac{J_1}{3}I\right)(a^1)^{1/3}\right)$$

where

$$J_1 = (a^1)^2 + (a^2)^2 + (a^3)^2 + 2,$$
$$J_2 = ((a^1)^2 + (a^2)^2 + (a^3)^2)^2 + 2 + 2(a^2)^2 + 2(a^3)^2,$$
$$G^2 = \begin{pmatrix} (a^2)^2 + (a^3)^2 + ((a^1)^2 + (a^2)^2 + (a^3)^2)^2 & a^2(1 + (a^1)^2 + (a^2)^2 + (a^3)^2) & a^3(1 + (a^1)^2 + (a^2)^2 + (a^3)^2) \\ a^2(1 + (a^1)^2 + (a^2)^2 + (a^3)^2) & 1 + (a^2)^2 & a^2a^3 \\ a^3(1 + (a^1)^2 + (a^2)^2 + (a^3)^2) & a^2a^3 & 1 + (a^3)^2 \end{pmatrix},$$
$$|G| = (a^1)^2.$$

Sound speed calculation in a simplified case ($w = 0$ and $a^3 = 0$) needs only components σ_{11} and σ_{12} and their derivatives. They read:

$$\sigma_{11} = -p - \frac{\mu}{3}\left(\frac{(a^2)^2 + 2((a^1)^2 + (a^2)^2)^2 - 2}{(a^1)^{1/3}} - 2((a^1)^2 + (a^2)^2 - 1)(a^1)^{1/3}\right),$$
$$\sigma_{12} = -\mu a^2\left(\frac{1 + (a^1)^2 + (a^2)^2}{(a^1)^{1/3}} - (a^1)^{1/3}\right).$$

The wave speeds v are solutions of the following polynomial:

$$(u - v)^4 + (u - v)^2\frac{(a^1)\sigma_{11,1} + \sigma_{12,2}(1 + (a^2))}{\rho} + (a^1)\frac{\sigma_{11,1}\sigma_{12,2} - \sigma_{12,1}\sigma_{11,2}}{\rho^2} = 0,$$

where

$$\sigma_{ij,\alpha} = \frac{\partial\sigma_{ij}}{\partial a^\alpha}.$$

These derivatives here read:

$$\sigma_{11,1} = -\frac{\partial p}{\partial a^1} - \frac{\mu}{3}(a^1)^{-2/3}\left(-\frac{1}{3}\frac{(a^2)^2 + 2((a^1)^2 + (a^2)^2)^2 - 2}{(a^1)^{2/3}}. + 8(a^1)^{4/3}((a^1)^2 + (a^2)^2) - \frac{2}{3}((a^1)^2 + (a^2)^2 - 1)\right),$$
$$\sigma_{11,2} = -\frac{\mu}{3}\left(\frac{(a^2)^2 + 8a^2((a^1)^2 + (a^2)^2)}{(a^1)^{1/3}} - 4(a^2)(a^1)^{1/3}\right), \sigma_{12,2} = -\mu\left(\frac{2(a^2)^2 + (1 + (a^1)^2 + (a^2)^2)}{(a^1)^{1/3}} - (a^1)^{1/3}\right),$$
$$\sigma_{12,1} = -\mu(a^2)\left(-\frac{1}{3}\frac{\left(1 + (a^1)^2 + (a^2)^2\right)}{(a^1)^{4/3}} + 2(a^1)^{2/3} - \frac{1}{3}(a^1)^{-2/3}\right).$$

With the EOS

$$p + p_\infty = e^{\frac{s - s_0}{C_v}}(a^1\rho_0)^\gamma$$

we also have:

$$\frac{\partial p}{\partial a^1} = \gamma\frac{e^{\frac{s - s_0}{C_v}}(a^1)^\gamma\rho_0^\gamma}{a^1} = \frac{\gamma}{a^1}(p + p_\infty)$$

References

[1] B. Despres, A geometrical approach to non-conservative shocks and elastoplastic shocks (preprint of HYKE)(2005).
[2] S.F. Davis, Simplified second-order Godunov-type methods, SIAM J. Sci. Stat. Comput. 9 (1988) 445–473.
[3] K.O. Friedrichs, P.D. Lax, Systems of conservation laws with a convex extension, Proc. Nat. Acad. Sci. USA 68 (1971) 1686–1688.
[4] P. Germain, Cours de Mécanique des Milieux Continus, Masson, Paris, 1973.
[5] S.K. Godunov, Elements of Continuum Mechanics, Nauka, Moscow, 1978 (in Russian).
[6] S.K. Godunov, E.I. Romenskii, Elements of Continuum Mechanics and Conservation Laws, Kluwer Academic Plenum Publishers, New York, 2003.
[7] H. Gouin, J.F. Debieve, Variational principle involving the stress tensor in elastodynamics, Int. J. Eng. Sci. 24 (7) (1986) 1057–1066.
[8] A. Harten, P.D. Lax, B. van Leer, On upstream differencing and Godunov-type schemes for hyperbolic conservation laws, SIAM Rev. 25 (1983) 35–61.
[9] A.G. Kulikovskii, N.V. Pogorelov, A.Y. Semenov, Mathematical aspects of numerical solution of hyperbolic systems, Chapman & Hall/CRC, 2001.
[10] G.H. Miller, P. Colella, A high-order Eulerian Godunov method for elastic–plastic flow in solids, J. Comput. Phys. 167 (2001) 131–176.
[11] G.H. Miller, P. Colella, A conservative three-dimensional Eulerian method for coupled fluid–solid shock capturing, J. Comput. Phys. 183 (2002) 26–82.
[12] F. Petitpas, E. Franquet, R. Saurel, O. Le Metayer, A relaxation-projection method for compressible flows. Part II: Artificial heat exchanges for multiphase shocks, J. Comput. Phys. 225 (2007) 2214–2248.
[13] J.N. Plohr, B.J. Plohr, Linearized analysis of Richtmyer–Meshkov flow for elastic materials, JFM 537 (2005) 55–89.
[14] J. Serrin, Mathematical principles of classical fluid mechanics, encyclopedia of physics, VIII/1, Springer-Verlag, 1959, pp. 125–263.
[15] R. Saurel, E. Franquet, E. Daniel, O. Le Metayer, A relaxation-projection method for compressible flows. Part I: The numerical equation of state for the Euler equations, J. Comput. Phys. 223 (2007) 822–845.
[16] V.A. Titarev, E.I. Romenskii, E.F. Toro, MUSTA-type upwind fluxes for nonlinear elasticity. Int. J. Numer. Meth. Eng., accepted for publication.
[17] E.F. Toro, M. Spruce, W. Speares, Restoration of the Contact Surface in the HLL-Riemann Solver, Shock Waves 4 (1994) 25–34.
[18] E.F. Toro, Exact and approximate Riemann Solvers for the artificial compressibility equations. Technical Report 97-02, Department of Mathematics and Physics, Manchester Metropolitan University, UK, 1997.
[19] J.A. Trangenstein, P. Colella, A higher-order Godunov method for modelling finite deformation in elastic–plastic solids, Commun. Pure Appl. Math. XLIV (1991) 41–100.
[20] B. Van Leer, Towards the ultimate conservative difference scheme IV. A new approach to numerical convection, J. Comput. Phys. 23 (1991) 276–299.
[21] M.L. Wilkins, Computer Simulation of Dynamic Phenomena, Springer, 1999.